BACHELOR

A study of the drying process of Pine sapwood with a NMR setup

Wassenaar, B.L.J.

Award date:
2014

A study of the drying process of Pine sapwood with a NMR setup

Bachelor End Project

B.L.J. Wassenaar

July 4, 2014

Supervisors:
Dr.ir. H.P. Huinink
Özlem Gezici, MSc

University of Technology Eindhoven
Department of Applied Physics
Transport in Permeabele Media
Cascade, 1.05

Abstract

Wood is a widely applicable material. It is however highly sensitive to external influence which will cause the wood to decay or even rot. A lot of companies nowadays study the behavior of coatings on wood to increase the durability of both wood and coating.

For studying and comparing the influence of coatings on moisture in porous material, NMR technique is ideal. It is non-destructive and can provide the information that is needed, such as the moisture content and its state. In this project, the first goal is to optimize the setup for measurements: for comparing the behavior of coatings against water sorption, it is necessary that moisture transport only takes places through the coating. The second goal is to describe the phases of the drying process of pine sapwood and to find a rough mathematical model.

For the first objective, two different types of sample holders are compared: it was concluded that a sample holder with a small inset gives the most reliable result. This optimization is done by investigating drying processes on pine sapwood. The second parameter studied is that if the sample needs extensive covering before putting the sample in the sample holder. It is proven that this is not needed, the sample holder itself is sufficient for performing measurements on coatings. However, the influence of the internal structure of the sample plays a big role in the drying process, more measurements with different samples should be performed for concluding that the sample doesn't need taping.

Experiments on uncoated pine sapwood provided enough information to describe 3 phases in the drying process of the wood. The first stage is homogeneous drying of the sample due to connections and alignment of the pores and cell walls. The evaporation rate is limited by external conditions. The second phase is the behavior and speed of the formed drying front. The third and last phase shows short homogeneous drying again, but now for the disappearing bound water. By optimizing parameters for drier samples, more information can be extracted and the last phase could be described more extensively.

At last, a rough mathematical model is provided for the second stage of drying. It uses Fick's law and a linear approximation is found. The drying front has a diffusion coefficient of $D=3*10^{-7}$ m^2/s. This is slower than just vapor diffusion of water in air ($D_{w,air} = 2.4 * 10^{-5}$ m^2/s) due to interactions of water with wood. The model is also applied to individual drying profiles, which showed a more curved behavior. The linear approximation is not bad, but the change in the diffusion coefficient should be taken into account.

Table of contents

List of abbreviations

FID – Free induction decay

FSP – Fiber Saturation Point

HSE – Hahn Spin Echo

OM – Optical microscope

M.C. – Moisture content

NMR – Nuclear Magnetic Resonance

RF – Radio-Frequency

RH – Relative Humidity

SB – Solvent borne (coating)

S.I. – Signal Intensity

SNR – Signal to Noise Ratio

TE – Echo time

TR – Repetition Time

VOC – Volatile Organic Compound

WB – Waterborne (coating)

1 Introduction

Wood has been used by human being for ages, but nowadays it is a material that has become indispensable. The usage started with weapons, tools and as a fuel for fire, but it was soon used for many more things. Today, wood is useful as a construction material for buildings, it is used in furniture and for paper. But it is also utilized in the arts; sculptures are made of wood, as well as frames of paintings, but also for music instruments and baseball bats.

That wood is widely applied, is clear. However, there is a major disadvantage of wood. It is highly sensitive to environmental influences like temperature. Furthermore, the presence of moisture in wood will cause degradation, such as wood rot. Complete prevention of the biological decay of wood is almost impossible, but the process surely can be decelerated. Deceleration can be achieved by applying a coating on the wood. Several studies already discussed many issues: van Meel discussed the efficiency of several coatings applied on different types of wood [1]. Donkers discussed the detection of free and bound water in wood, but he also told about the effect of different particle sizes of the pigment in coatings and discussed the ageing of the coatings [2].

Both of the studies used the principle of nuclear magnetic resonance (NMR). It is a way to non-destructively measure the moisture content in a porous medium, such as wood. However, because of the behavior of wood during sorption processes like shrinking and swelling, handling the sample becomes crucial and the sample holder should be adjusted to the changes which wood is going through during such a process. Van Meel already found that the sample holder highly influences the drying measurements and recommended that these holders still need some optimization, which will be the first objective of this study.

This study is about the drying process of pine sapwood. Drying measurements on woods started about 30 years ago; Menon used in 1987 already NMR techniques for the drying process on wood [3]. Wood and its drying behavior is also studied above and below the fiber saturation point of wood with methods like CT-scanning with weighing and with X-ray scattering, respectively [4] and [5]. Comparing coatings with NMR setup is something that came up the last few years: Donkers and Van Meel are good examples of researching this trend.

The second aim of this study is about modelling the drying process of uncoated pine sapwood. Modelling the drying behavior gives a good insight about the drying process. When these phases of drying can be quantified, the quantifications can help in later studies for, for instance, the modelling of drying processes of coated wood. A mathematical approach is also taken for the behavior of the drying front. Stanish provided in 1986 a mathematical model of drying for hygroscopic porous media like wood [6]. Furthermore, not really much is researched yet in modelling the drying process of wood.

Chapter 2 will include the specifications of the wood and the samples, chapter 3 will introduce the world of NMR and the usage of NMR on wood. Chapter 4 will contain the optimization of the setup, while chapter 5 will provide the models. Chapter 6 contains the conclusions and recommendations.

2 Wood & samples

2.1 General introduction

When it comes to wood, many properties emerge. It is a very complex material, mostly because of its structure. Those properties ensure that the behavior of moisture in timber gets even more complicated. However, this behavior can be adapted with coatings. The structure of wood, moisture behavior and the coatings are respectively discussed in the next paragraphs. After these, the used samples in the project will be discussed.

2.1.1 Structure

Wood is an anisotropic and inhomogeneous material. This is because 90 to 95% of the cells are elongated and parallel to the tree trunk. The remaining 5 to 10% of the cells are arranged in radial directions. The cell walls mainly consist of cellulose, hemicellulose and lignin. In Figure 2-1 is a schematic representation shown of the trunk of a tree.

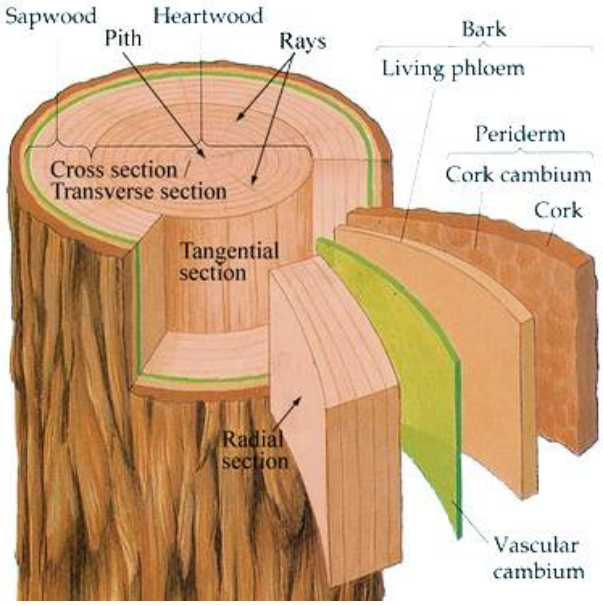

Figure 2-1: Schematic representation of the trunk of a tree. This picture is subtracted from [7].

As can be seen, a tree consists mainly of two types of wood: the heartwood and the sapwood. Heartwood can be regarded as dead wood, while sapwood is the living wood: it conducts water from the roots to the leaves and supplies minerals. Furthermore, the different sections can be distinguished: radial, transversal and tangential. The behavior of wood depends on the direction of the cut, as can be explained by the anisotropy. Moreover, rays and pits are present in the wood. The utility of these are discussed in the next sections. Additionally, there are two types of wood: softwood and hardwood. These types will also be discussed in the next paragraphs.

2.1.1.1 Hardwood

A universal structure of hardwood is difficult to provide, there are a lot of variations in it, depending on the type of tree. However, hardwood exists of vessels, fibers and wood rays. The vessels and fibers are parallel to the direction of growth, the vertical direction, while the rays are aligned in the radial direction. Water mostly flows in the growth direction; transport in the transversal and radial direction is nevertheless also possible. Not through the cell walls, the vessels and fibers are impermeable, but the transport takes place through pits. These pits are small gaps in the cell walls and connect the lumen, the 'empty space' inside the cell wall, with each other. In Figure 2-2 (b) is a schematic representation of hardwood shown.

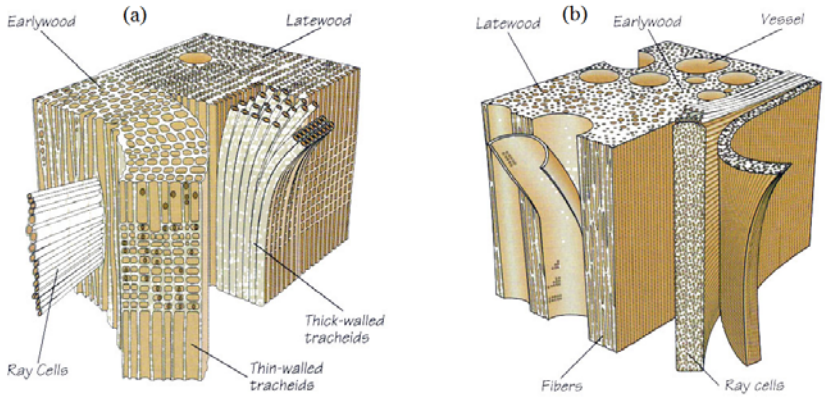

Figure 2-2: Schematic representation of the structure of (a) softwood and (b) hardwood. This picture is subtracted from [8].

2.1.1.2 Softwood

For softwood, the structure is easily described. The structure is formed by tracheids, longitudinal cells, which are relatively longer than the vessels in hardwood. In the radial direction there are ray tracheids or ray cells. Again, moisture transport in transversal direction takes place through pits. In early wood, the walls of the tracheids are thin, while they are thicker in the latewood. However, the volume of the ray cells is around 7%, while for hardwood this is around 17%. In Figure 2-2 (a) is the schematic representation of softwood shown. What can be observed is a large canal in the latewood. This is called a resin canal, intercellular space, which transports resin. In Figure 2-3 the difference between early tracheids and late tracheids is really clear: the thicker walls are the late tracheids, while the early tracheids are very wide and thin walled. The picture is made with an Optical Microscope (OM).

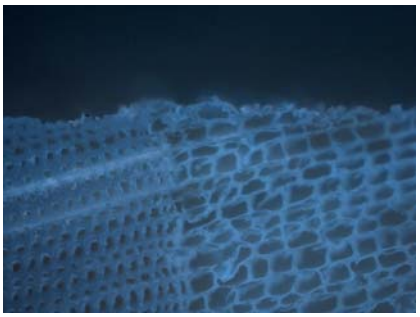

Figure 2-3: An optical microscope picture of Pine Sapwood. The early tracheids are at the right, the late tracheids at the left.

2.2 Moisture in (Pine sap)wood

The amount of water present in wood is called the moisture content (MC). The MC can be calculated by

$$MC = \frac{m_{sample} - m_{ovendried}}{m_{ovendried}} \cdot 100\% \tag{1.1}$$

Where m is the mass in kilograms. The oven dried mass of the wood is measured after drying in an oven of 105 ± 3 °C for 1 day (after 3,5 day it gives the same result), and the mass of the sample is the mass of the wood with water. Moisture is drawn into timber because of interaction with the water in air. The amount of water present in the air is the relative humidity (RH), which is defined as

$$RH = \frac{p}{p_0} \cdot 100\% \tag{1.2}$$

Where p is the partial vapor pressure of water in air and p_0 is the associated saturated pressure. The equilibrium MC at a certain relative humidity differs per wood species. In Figure 2-4 is the sorption curve of Pine Sapwood shown.

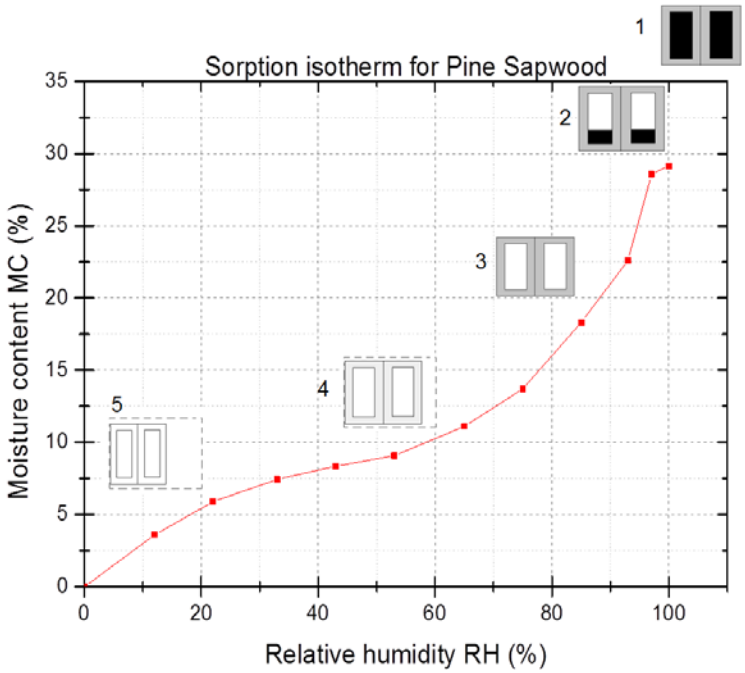

Figure 2-4 Sorption curve for Pine Sapwood, together with the phases of the cell associated with the curve.

Together with the isotherm, the equilibrium MC per RH at a certain temperature, the behavior of the cells with the moisture is shown. When the drying process is considered, the curve must be followed from top to bottom. When wood is fully saturated, the cell walls are saturated and have reached their maximum of swelling. The lumina are fully occupied with water (1). When the wood starts to dry, the lumina will lose their water content first (2). When they are completely empty, the fiber saturation point (FSP) is reached (3). This is the point where the fibers in the cell

walls are fully saturated with water, and mainly occurs at 98% RH. This water is called *bound water*; it is bound to and between cellulose fibers. The water which was present in the lumina is *free* or *unbound water*. However, with more drying of the wood after the FSP, the cell walls will lose water which will cause shrinkage of the wood (4). When it is completely dry (oven dry), no water is present in the wood (5).

The transport of moisture in wood can be summarized: In the radial and transversal direction the transport can take place through minor pits in the cell walls. This transport through pits is called vapor diffusion and moisture transport within a cell wall is diffusion. The unbound moisture behaves differently in soft- and hardwood, because of their difference in structure. In softwood is the influence of rays much higher. In hardwood, vessels are the most permeable flow paths in the longitudinal direction when they are not occluded.

2.3 Coatings

Information about the coatings is obtained from [9].

A coating is a covering that is applied to the surface of the wood. It can be applied for decorative of functional reasons. It can be used for adhesion, wettability, resistance against corrosion or just wear resistance. A coating normally has the next three components:

Binders or resins: a material that holds the other materials together to form a cohesive matrix. It will form a film which will protect the wood against, for example, moisture.

The main binders are based on acrylics and alkyds. Acrylics attribute a lot to the resistance to hydrolysis; alkyds are easily applied under variable conditions and form a flexible coating.

Carrier solvents: water or organic solvents with the purpose to transfer the other ingredients to the surface of the wood and allow the formation of a film.

Coatings for wood were usually made with solvent borne carriers. However, legislation changed a lot over the past decades. Solvent borne coatings contain a lot of Volatile Organic Compounds (VOC's), which are harmful for the environment. Applying a solvent borne coating (SB) will cause the solvent to evaporate and after that, oxidative cross linking appears. Improvement of waterborne coatings, which contain less VOC's, is favorable. When a waterborne coating (WB) is applied, first the polymers will start to coalescence. If the temperature is high enough, the water will evaporate, which will restrict the polymers for movement.

Pigments: Mainly used for decorative purposes. It can add color, but it can also protect the wood against photo degradation.

2.4 Samples

The samples used in this project are pine sapwood. The samples are made with a radial cut and are cylindrical: they have a height of 10 mm and a diameter of 20 mm. When they have a high MC, the sample swells 11% in height, 5% in perpendicular to the fibers and almost nothing parallel to the fibers. These results can be seen in Figure 2-5.

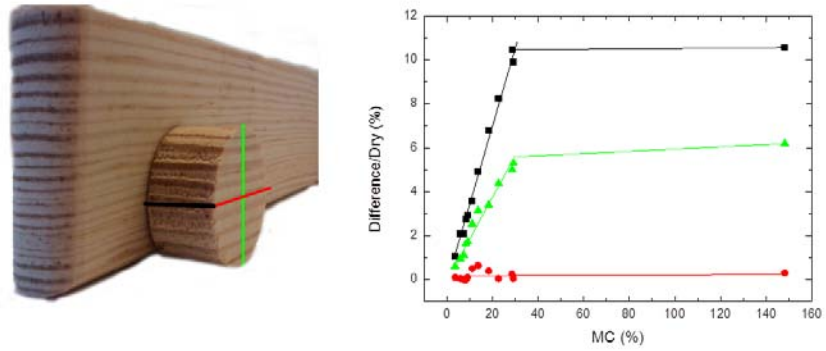

Figure 2-5: At the left is the pine sample as specified, in green black and red are the directions indicated. In the graph, these colors match with the amount of swelling.

There are four types of samples used:

- Pine sapwood with no coating (Uncoated)
- Pine sapwood coated with a waterborne acrylic coating (WB Acrylic)
- Pine sapwood coated with a waterborne alkyd coating (WB Alkyd)
- Pine sapwood coated with a solvent borne alkyd coating (SB Alkyd)

The coated samples have on the bottom an extra coating; a very thick completely impermeable coating. This is in order to protect the bottom against the weathering, which is for preparing the coatings. The coatings were first applied by brushing and then the samples are sanded. The wood will be slightly penetrated and the surface will end up plain. This is to make sure that when after this the coating is applied again, it will have the same thickness everywhere. After sanding, the coating is applied twice so the thickness of the whole coating is eventually 50 µm. This can be seen in Figure 2-6, an image which is made with an OM just like Figure 2-3, where the coating is visible. The visible sample is Pine sapwood with an SB Alkyd coating, which is thicker than the intended 50 µm.

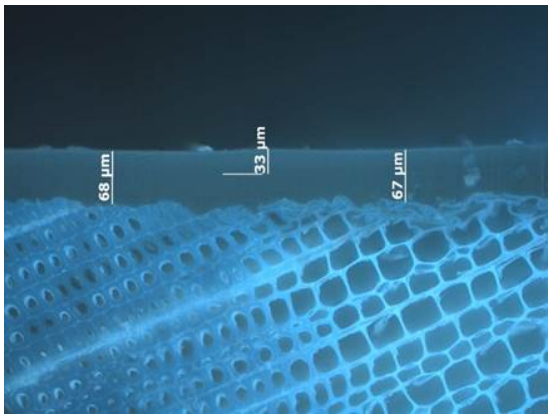

Figure 2-6: An OM-made image of Pine sapwood with a solvent borne alkyd coating.

For this project, only the drying process is studied. For that purpose, the samples are saturated by putting them in the water for 2 to 4 weeks and the 2nd step is putting them in the sample holder. The samples are punched out a larger piece of the wood, with the same coating. The preparation, the punching as well as the saturation, is shown in Figure 2-7.

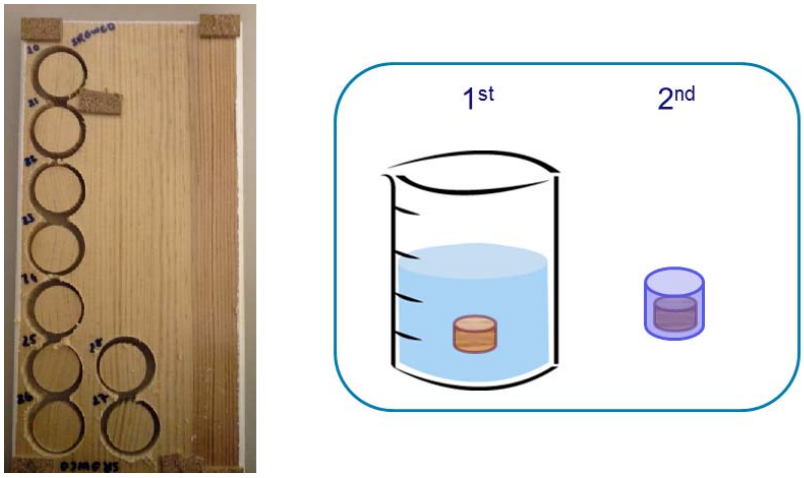

Figure 2-7: Sample preparation, first the sample is punched out a bigger whole and after that put in water for 2 to 4 weeks. After saturation, the samples are used for drying and are put in the sample holder. The shown wood is Pine sapwood with a WB Acrylic coating.

If the knowledge about the structure of pine sapwood, which is softwood, the information about the moisture in wood and the sample are all brought together, the influence of the geometry and pore sizes on the moisture transport can be discussed:

The way the sample is cut highly influences the water transport in the sample. In Figure 2-8, the directions are showed. Moisture transport is really quick in the transverse direction (red), because that is the direction of the longitudinal cells. In the living tree, these are the cells that transport the water from the roots to leaves. In the green direction are ray cells. These cells lay in the radial direction (green) and in the tree it conducts water and saps in the lateral direction. If a cross section is made of the tree, these ray cells will look like the spokes of a wheel. They will transport moisture in the sample slower than the tracheids, but transport is still easy. In the transverse direction (black) the water transport takes places through pits: small gaps in the cell walls of the longitudinal cells. This transport is relatively slow, and depends on the inner structure of the wood. Of the cells and cell walls are aligned, transport is quicker when the cells and cell walls are not aligned. The three different kinds of behaviors can be linked to the swelling: for different transport routes, the sample swells differently.

In the case that a sample is cut a little bit skew in one direction, the measured moisture transport will differ: One of the types of water transport will get a higher influence. In the showed figure, transport will be slow, because the transport is mainly in the transversal direction. If these fibers are however skew, the moisture transport should be described as a combination of transversal transport and radial transport.

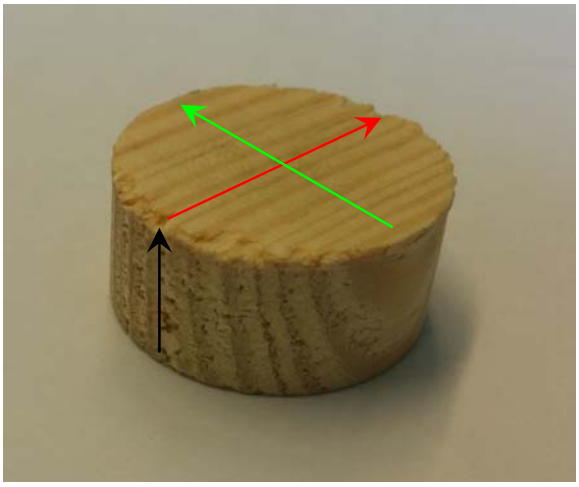

Figure 2-8: A sample with the directions in colors: Red is growth direction, green is the radial direction and the black one is the transversal direction.

3 Nuclear Magnetic Resonance

Nuclear Magnetic Resonance (NMR) was first described and measured in 1938 and eventually two Nobel Prizes were won in this field of research. It has several applications because it is a non-destructive method. NMR is applied in the medical world for imaging (Magnetic Resonance Imaging, MRI), but also in the chemistry. Chemists can determine the structure of many compounds by studying the peaks of NMR spectra. Benefits of NMR are furthermore that measurements can be made through time and depth, which are both really useful when measuring porous media, such as wood.

In this chapter not only the theory of NMR, paragraph 3.1, will be shortly discussed, but also the NMR technique applied to wood. What sequences are used and how the free and the bound water can be distinguished will be made clear.

3.1 Theory

NMR is a physical phenomenon in which a nucleus in a magnetic field absorbs and re-emits electromagnetic radiation. The energy of the radiation has a certain resonance frequency and depends on the strength of the magnetic field and the magnetic properties of the isotope of the atoms. The commonly used nucleus is ^{1}H.

3.1.1 Nuclear spin and magnetic moment

A nucleus of an atom is composed by neutrons and protons. These neutrons and protons have an intrinsic quantum property 'spin'. The total spin of a nucleus will therefore be the combination of all the spins of the neutrons and protons. There are several rules for combining these spins, like the exclusion principle of Pauli which states that two particles cannot occupy the same state. This will eventually lead to nuclei with spins I = 0, ½, 1, 3/2 etcetera. Because of this spin, a quantum effect occurs; the nucleus will gain an intrinsic magnetic moment. This moment is defined as

$$\vec{\mu} = \gamma \hbar \vec{I} \tag{1.3}$$

, where γ is the gyromagnetic ratio, the ratio of its magnetic dipole moment to its angular momentum, which Hornak described [10]. All theory in this paragraph is also from Hornak, as well as the sequences. For ^{1}H, the gyromagnetic ratio is γ = 42.56 MHz/T. The magnetic moments together are equal to the magnetization M:

$$\vec{M} = \sum_i \vec{\mu}_i \tag{1.4}$$

When a nucleus is placed in an external static magnetic field B_0 that is not aligned with the magnetic moment, a torque τ on the nucleus will arise:

$$\vec{\tau} = \vec{\mu} \times \vec{B}_0 \tag{1.5}$$

This torque will cause the magnetic moment to precess around the magnetic field. This precession is called the Larmor precession and has a Larmor frequency ω_L:

$$\omega_L = \gamma \left| \vec{B}_0 \right| \tag{1.6}$$

Bloch stated the following differential equation:

$$\frac{d\vec{\mu}}{dt} = \gamma\vec{\mu} \times \vec{B}_0 \tag{1.7}$$

3.1.2 Rotating frame

As can be deduced from the above equations, the frame in which everything is observed and calculated is not very adequate. Therefore, a rotating frame of reference is introduced. The coordinates in the rotating frame are designated by (x′,y′,z′) and the laboratory frame with (x,y,z). The introduced rotating frame will rotate around the z-axis, so z′=z, with the Larmor frequency ω_L. When an arbitrary vector *r* in the laboratory frame is considered, the next follows for the rotating vector *r′*:

$$\frac{\partial\vec{r}\,'}{\partial t} = \frac{d\vec{r}}{dt} - (\vec{\omega}_L \times \vec{r}) \tag{1.8}$$

In this equation, d/dt is the derivative in the stationary frame and $\partial / \partial t$ is the derivative in the rotating frame. For the magnetic moment this yields

$$\frac{\partial\vec{\mu}\,'}{\partial t} = \frac{d\vec{\mu}}{dt} - (\vec{\omega}_L \times \vec{\mu}) \tag{1.9}$$

If this is now combined with the Bloch differential equation (1.10), this will lead to

$$\frac{\partial\vec{\mu}\,'}{\partial t} = \gamma\vec{\mu} \times \vec{B}_0 - (\vec{\omega}_L \times \vec{\mu}) = \vec{\mu} \times (\gamma\vec{B}_0 - \vec{\omega}_L) \tag{1.10}$$

But known is that $\partial\vec{\mu}\,'/\partial t$ will be equal to zero because $\vec{\omega}_L = \gamma\vec{B}_0$. This shows that the precession of the nucleus due to the magnetic moment is not observed in the rotating frame. With this frame, nuclei can be manipulated with a secondary magnetic field B_1. The nucleus will now precess around this field, with ω_1 as angular frequency. When B_1 is applied for an short amount of time t_p, the magnetic moments will be flipped over an angle

$$\theta = \left|\vec{\omega}\,'_1\right| t_p = \gamma \left|\vec{B}\,'_1\right| t_p \tag{1.11}$$

3.1.3 Magnetization

In NMR experiments, only the net magnetization *M* matters instead of the individual magnetic moments μ. When applying a pulse with the secondary field B_1 as described above, the equilibrium state of M_0 along B_0 at the z-axis will be disrupted and the magnetization *M* will be rotated in a different direction. As expected, the magnetization will slowly recover to its equilibrium state. This recovering is due to longitudinal and transverse relaxation.

The longitudinal relaxation is also called spin-lattice relaxation and has a corresponding relaxation time of T_1. It stands for the restoring of the magnetization vector along the B_0 field. The transverse relaxation is also called the spin-spin relaxation and has a corresponding relaxation time of T_2. This is a quantification of how fast the magnetization perpendicular to B_0 goes to zero. The Bloch equations are now

$$\frac{dM'_{x'}}{dt} = -\frac{M'_{x'}}{T_2} + \gamma(\vec{M}' \times \vec{B}_1')_{x'}$$
$$\frac{dM'_{y'}}{dt} = -\frac{M'_{y'}}{T_2} + \gamma(\vec{M}' \times \vec{B}_1')_{y'} \qquad (1.12)$$
$$\frac{dM'_{z'}}{dt} = -\frac{M'_{z'} - M_0}{T_1} + \gamma(\vec{M}' \times \vec{B}_1')_{z'}$$

Most of the sequences uses flip angles of 90° and 180°. Therefore, an example of both cases is given. Start with $M(t<0) = (0,0,M_0)$ and apply B_1 at t=0 until the flip angle θ = 90°/180°. The magnetization M will now be respectively $M_{90°} = (M_0,0,0)$ and $M_{180°} = (0,0,-M_0)$. These experiments will give the following solutions to the Bloch equations mentioned above for the 90° pulse,

$$M'_{x'} = M_0 \cdot \exp(-t/T_2)$$
$$M'_{y'} = 0 \qquad (1.13).$$
$$M'_{z'} = M_0(1-\exp(-t/T_1))$$

And for the 180° pulse:

$$M'_{z'} = M_0(1-2\cdot\exp(-t/T_1)) \qquad (1.14).$$

3.1.4 Spatial resolution

In order to obtain position-specific data with NMR, a gradient is applied. For 1-dimensional resolution, this gradient usually lies in the z-direction. The magnetic field will now be

$$\vec{B}(z) = (0,0,B_0 + z\cdot G_z) \qquad (1.15),$$

Which will yield the Larmor frequency

$$\vec{\omega}_L = \gamma\left|\vec{B}\right| = \gamma(B_0 + z\cdot G_z) \qquad (1.16).$$

And this shows that the Larmor frequency is now position dependent. When measurements are performed, the frequency will be measured. After applying a Fourier transform, this can easily be converted to a position with that gradient. The resolution of the results will now be

$$\Delta z = \frac{2\pi}{\gamma G_z t_w} \qquad (1.17),$$

Where t_w is the acquisition time or the window width. With small relaxation times,

t_w must be replaced by T_2^*, a quicker type of T_2-relaxation due to field inhomogeneities. As can be deduced from the formula, the spatial resolution is limited by the gradient and the acquisition time. When performing measurements, not only the spatial resolution must be taken into account, as well as the Signal to Noise Ratio (SNR)

$$SNR \propto \sqrt{\frac{N_{avg}}{t_w}} \quad (1.18),$$

Where N_{avg} is the number of averages in one measurement. If this SNR is not high enough, the signal cannot be distinguished from the noise, even if the spatial resolution is high.

3.2 NMR & Wood

The theory of nuclear magnetic resonance is explained in the previous paragraph. In this paragraph, the usage of NMR on the wood is discussed. First, the used sequences will be explained, together with the interpretation of the measured signals. Secondly, the use of relaxation times for the distinction between the free and bound water will be explained. Lastly, the calibration will be showed.

3.2.1 Sequences

3.2.1.1 Free Induction Decay

For understanding the NMR signal and processing, the most understandable sequence is the free induction decay (FID). A schematic representation of the FID is given in Figure 3-1.

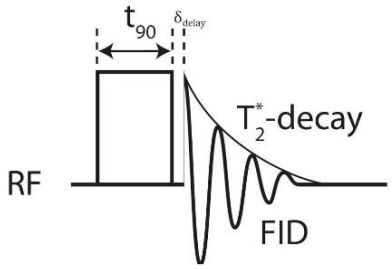

Figure 3-1: The free induction decay sequence. The measured FID signal decays with T_2.*

The pulse of the external B_1-field is done with a coil and is called a RF-pulse, a radio-frequency pulse. The duration of the pulse t_{90} is the amount of time it takes to flip the net magnetization 90°. Because of a short delay in the system δ_{delay}, it is not possible to measure the FID signal directly after the pulse. This is due to the fact that the signal is measured with the same coil as with the RF pulse was given with. The FID signal decays with T_2*, which is explained in the next formula:

$$\frac{1}{T_2*} = \frac{1}{T_2} + \frac{1}{T_2'} \quad (1.19)$$

As can be seen, T_2* is faster than T_2 due to field inhomogeneities incorporated in T_2'.

3.2.1.2 Hahn Spin Echo

What can be seen in the FID described above is that the signal decays really fast due to field inhomogeneities. The loss of signal that is caused by this phenomenon can be counteracted with a Hahn Spin Echo (HSE). A schematic representation of the HSE is shown in Figure 3-2.

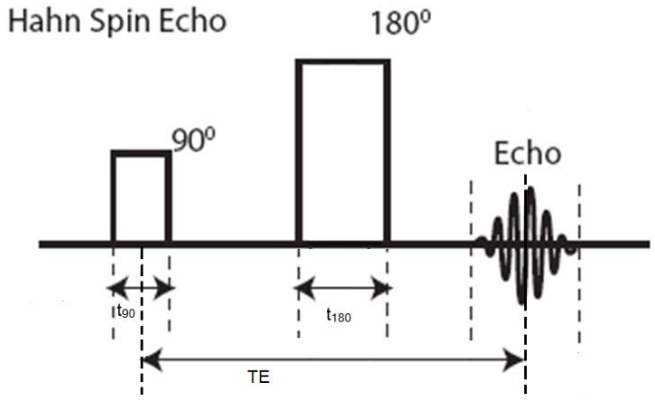

Figure 3-2: Schematic representation of a Hahn Spin Echo sequence. Consecutively a 90° and a 180° pulse, then an echo measurement. Time between de first pulse and the echo is the Echo Time (TE).

In Figure 3-2, TE is the echo time, the time between the 90° pulse and the echo. If the echo time is too short, the measurement will be too quick after the 180° pulse and the beginning of the echo will be missed. If the echo time is too long, it may be that the signal has decayed that the amplitude is too small.

The explanation of the HSE is done on the basis of Figure 3-3.

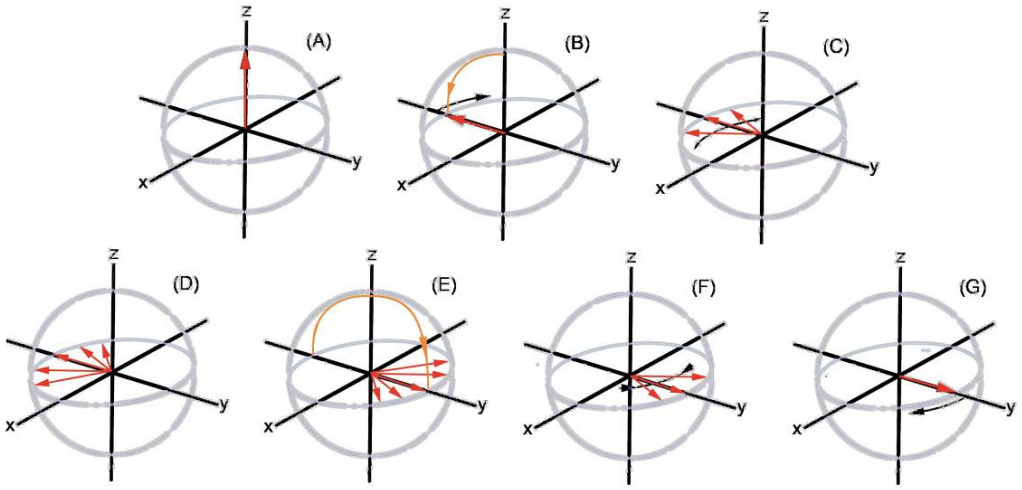

Figure 3-3: A visualization of the magnetization vectors during the Hahn Spin Echo Sequence.

The magnetization is aligned to the B_0 field in the z-direction (A). Then a 90° is applied, which brings the magnetization to the –y-axis (B). The spins will dephase (C), (D) and is the FID described above. Thereafter, a 180° pulse is applied (E). The spins will now be brought in phase again (G). The measured echo contains the phasing (G) and the dephasing after G.

The HSE is used in this project to develop the moisture content profiles during the drying measurements. According to

$$MC(NMR) = 100 \times \frac{S.I._{corrected} * V_{sample}}{m_{ovendried}} \cdot \rho_{water} \qquad (1.20)$$

it is possible to deduce from the corrected S.I the moisture content. The corrected signal intensity is the intensity of the echo after a reference is applied, which will be explained in section 3.2.4.. Except for this S.I., the volume of the sample V_{sample} in dm^3 and the oven dried mass of the sample $m_{ovendried}$ in kg are needed for the conversion. The density of water, ρ_{water}, is equal to 1 kg/dm^3 and is therefore not used in calculations.

However, a Hahn Spin Echo sequence only returns the amplitude of the direct measured echo. If the T_2 relaxation time is needed, then a different sequence is more sufficient, as described in the next paragraph.

3.2.1.3 CPMG sequence

The CPMG sequence, named after Carr, Purcell, Meiboom and Gill, is a multiple spin echo sequence. A schematic representation of the CPMG sequence is shown in Figure 3-4.

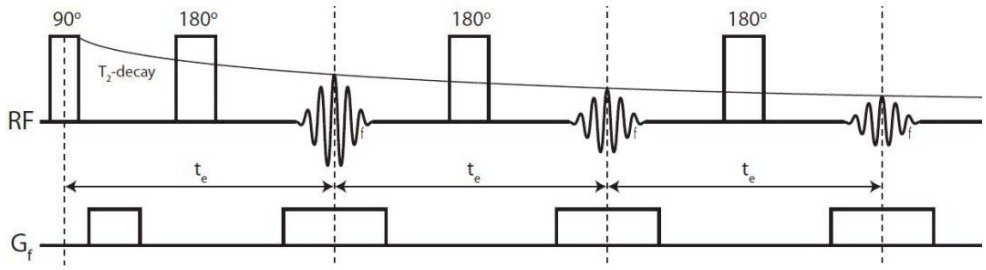

Figure 3-4: A CPGM sequence. It starts with a 90° pulse and then a train of consecutive a 180° pulse for refocusing and an echo. The train of echoes is decaying with T_2.

A CPMG sequence is just a Hahn sequence, but with a train of 180° pulses and echoes afterwards. The amplitudes of the echoes decay with T_2 as a time constant. The refocusing 180° pulses ensure that the field inhomogeneities have no consequences on the system. The decay of the signal is

$$S = \rho e^{-nTE/T_2}(1 - e^{-TR/T_1}) \tag{1.21}$$

According to Bloch. TR is the repetition time, the time between the 90° pulses. When multiple types of T_2 are present, the signal intensity then decays multi-exponentially

$$S = \sum_i S_i e^{-nTE/T_{2,i}} \tag{1.22}$$

Or when the time distribution is continuously, (1.22) will be an integral.

The gradient pulses G_f in figure 3-4 is needed to measure a 1D NMR signal, instead of 0D. This way, the sample does not have to be moved to gather all the information. This will be further explained in the next paragraph about slice selection.

The CPMG sequence can be used for a T_2-relaxation time analysis of the behavior of the moisture in wood. Elaboration on this is done in section 3.2.2.

3.2.2 Relaxation time & moisture content in wood

As stated in paragraph 3.1.3, the T_2 relaxation time is the spin-spin relaxation time. It is therefore consistent with the fact that T_2 is specific per material, because the spin-spin interaction will be different. For moisture in wood, this means that the difference between bound and free water is visible in the measurements. The distinction between free and bound water is first mentioned by Menon *et al*, 1987 [3]. A visualization of this is shown in Figure 3-5.

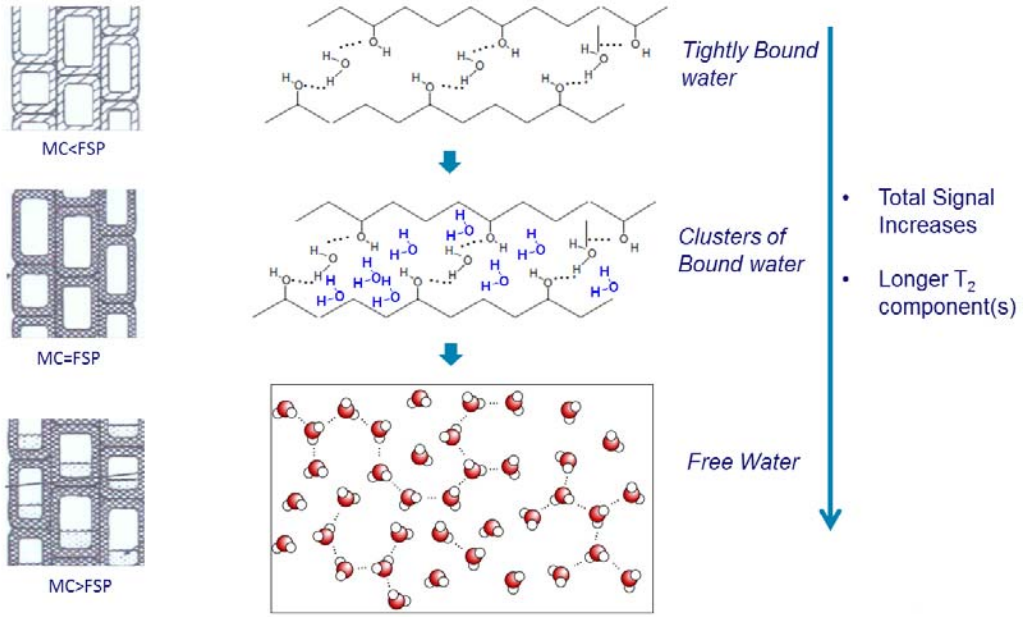

Figure 3-5: The differences in the water molecule bonding in the bound and free water. From top to bottom, the total signal increases. Moreover, the T_2*-relaxation time increases because of that bonding.*

In Figure 3-5 it is clear that tightly bound water, clusters of bound water and the free water have a different T_2-relaxation time. However, it is conceivable that the difference of relaxation time between the tightly bound and the clusters of bound water is much smaller than the difference between the bound and free water. In the first situation, only a small separation of the relaxation time is observed. In the second case, bound and free water appear separately in a T_2-profile.

For clarification, a typical T_2 decay graph is shown, together with a T_2 profile, in Figure 3-6.

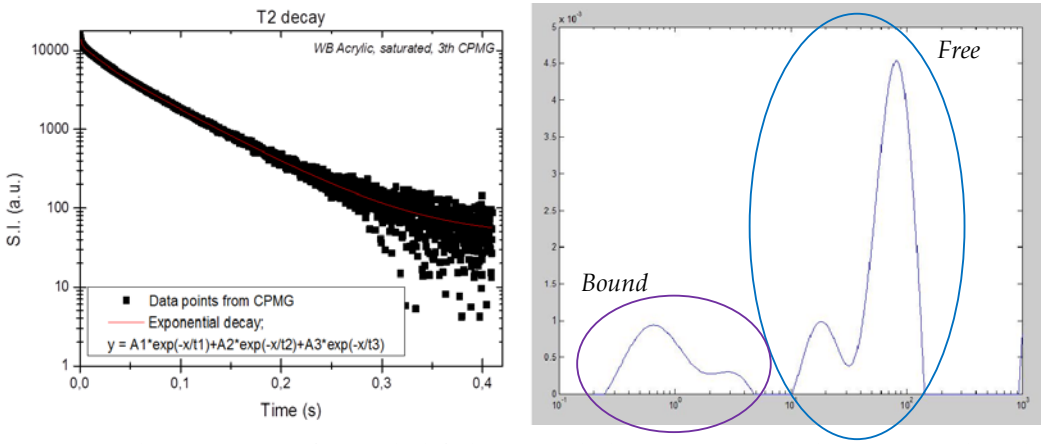

Figure 3-6: Characterization of T_2; at the left the decay which is measured with the CPMG, at the right a possible corresponding spectrum of the T_2 relaxation times. The purple ellipse presents the bound water, while the blue one circles the free water.

At the left in the figure, the T_2 decay is shown. The decay is a multi-exponential decay. In the shown graph, it is fitted with 3 parameters, while it should actually be 4, as can be seen in the right graph. What becomes clear in the profile at the right, is the distinction between the bound and the free water. T_2-relaxation times that are in the order of a few milliseconds are bound water, first mentioned by Arauju *et al* in 1992 [11]. Relaxation times that have an order of magnitude of 10 ms is free water, which is found by Menon *et al*, 1989 [12]. For the free water, two peaks are observed. These are most likely due to different pore sizes in Pine Sapwood. Menon also stated that the T_2 – value for moisture in earlywood tracheids is around 100 ms, while the latewood tracheids give a value of 50 ms. For bound water, two peaks appear as well due to the difference in the thickness of the cell walls in early- and latewood tracheids. An interesting thing to regard is what happens during drying. An example of that is shown in Figure 3-7.

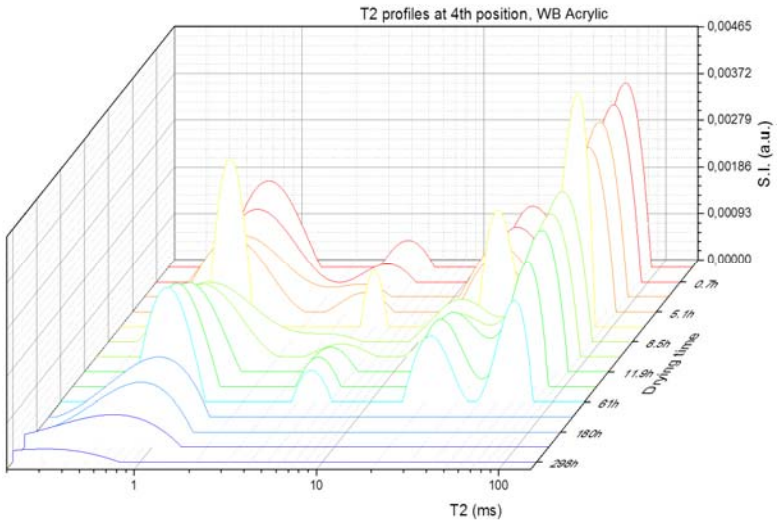

Figure 3-7: T_2 profiles during drying time. After a while, the free water is gone and the bound water is also decreasing. A shift in the T_2 of bound water is also observed.

Comparing typical figures like this with drying profiles gives a clear idea of what happens in a wood sample. This will be further discussed in Chapter 5.

3.2.3 Slice selection, settings, calibration & reference

3.2.3.1 Slice selection

Applying a gradient, as stated in section 3.2.1.3, gives the probability of measuring a 1D profile, which is also shown in equation (1.16). It states that the Larmor frequency is dependent of the position where the measurements are done. The obtained resolution is presented in (1.17). In this project, the center of the sample is aligned with the center frequency of the setup. This was f_{before} = 31.002 kHz before a shutdown of the power in the lab, and after that it is: f_{after} = 30.9968 kHz. So the sample is 5 mm below this frequency and 5 mm above this frequency. When a range of frequencies is applied during the measurement, several slices of the sample can be measured without moving the sample. The frequency can be converted to a position with the applied gradient. The settings, including the gradient, are further explained in the next section.

3.2.3.2 Settings

The NMR that is used produces a field of 0.75 T. Two sequences are used, the Hahn Spin Echo and the CPMG sequence, both explained in section 3.2.1. The HSE is used for making the profiles, the CPMG sequence can be used for the T_2 analysis. The parameters for this sequence are displayed in Table 3-1. These parameters are the ones that determine the SNR and therefore the accuracy of the moisture content profiles. These parameters are optimized for wood samples that contain a lot of water.

Table 3-1: Measurement parameters for the Hahn Spin Echo and the CPMG pulse sequence.

	t_e (µs)	WW (µs)	N_{avg}	N_{CPMG}	$Freq_{range}$ (kHz)	N_{freq}	G_z (mT/m)	$t_{90°}$ (µs)	TR (s)
HSE	200	120	4	-	280	37	418.5	25	8
CPMG	200	120	32	2048	160	7	418.5	25	8

The echo time t_e is the time between the 90° pulse and measuring the echo. The window width *WW* is the duration of measuring the echo. N_{avg} is the number of averages, N_{CPMG} is the number of 180° pulses (and therefore the number of echoes) during the CPMG sequence. $Freq_{range}$ is the range of frequencies used for the slice selection, as explained in section 3.2.2.The repetition time TR is the total time for a whole sequence. The duration of the 90° pulse $t_{90°}$ is determined by equation (1.11). For the 180° pulses, the duration is $t_{180°} = 2 * t_{90°}$, and the power is not amplified.

Furthermore, a gradient G_z is used, as can be seen in the table. This gradient is used for converting the frequency to a position in the sample. The calibration of the gradient is shown in Figure 3-8.

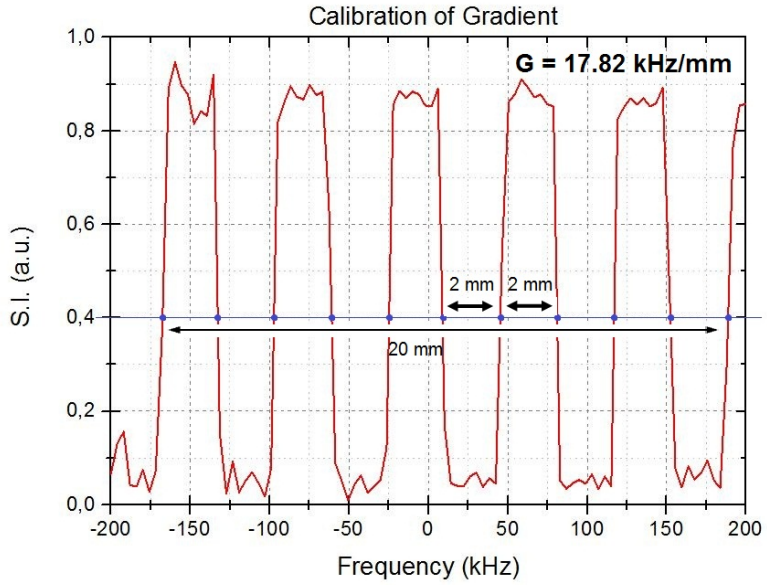

Figure 3-8: The calibration of the gradient. A gradient of G=*17.82 kHz/mm is deduced.*

For the calibration, a holder is used with alternating 2 mm of $CuSO_4$ and 2 mm of Teflon, which gives no signal. A gradient of G=17.82 kHz/mm is deduced.

3.2.3.3 Calibration

For interpreting and quantifying the measured signals from the NMR, a calibration is needed. For the wood, this starts with relating the measured signal intensity S.I. to the moisture content. The M.C. can be determined in two ways. The first one is calibrating by weighing the sample with different R.H. and therefore with different moisture contents, as described by the sorption isotherm, and measure the signal intensity. The associated graph is shown in Figure 3-9. The mass of the oven dried sample is $m_{ovendried}$ = 1650 mg and the volume of the sample is V_{sample} = 10^{-6}π m^3.

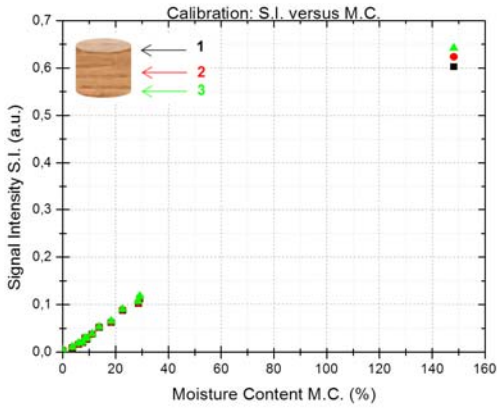

Figure 3-9: Calibration of the signal intensity to the moisture content. The related formula is given.

Secondly, the M.C. can also be calibrated by preparing the sample at different R.H. and measure the signal intensity directly. From the T_2 – analysis, the moisture content can be deduced. This measured moisture content is denoted as M.C.(NMR). It can also be calculated with equation (1.20).

Below the fiber saturation point however, these two moisture contents are not the same. Above the FSP, all the signal is measured what can be seen in the relaxation analysis. Below this point, signal will be lost due to the fact that the T_2-relaxation times are smaller than the echo time. Therefore, the measured M.C. will deviate from the weighted M.C.. A correction on the measured M.C. is needed and this calibration is shown in Figure 3-10. The difference between the two moisture contents is a factor 1.065, which is really small.

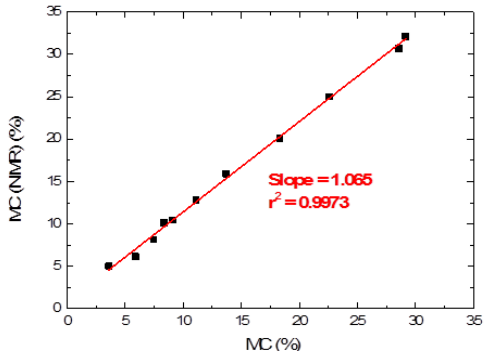

Figure 3-10: The calibration of the M.C.(NMR) against the M.C. for moisture contents below the FSP.

The sorption isotherm, already shown in section 2-2, is also necessary in the calibration part. Samples can be prepared at different R.H., but the M.C. of a sample can't be controlled easily.

3.2.3.4 Reference

A reference is needed before and after every measurement, to check whether nothing happened with the settings or setup during the measurements. In addition, it is needed because the setup is not equally sensitive at every frequency. This sensitivity needs correction with the reference, which is shown in Figure 3-11. At the left of the figure, only the profile of the reference is showed. In the middle is the uncorrected signal, the signal not divided by the reference. At the right is the corrected signal, which shows a proper profile of a saturated sample. The used reference in this project is a holder completely filled with a solution of copper sulfate, $CuSO_4$, in water. Copper sulfate is used because it lowers the T_1 relaxation time of water, which lowers the duration of the measurement of the reference and therefore speeds up the measuring process.

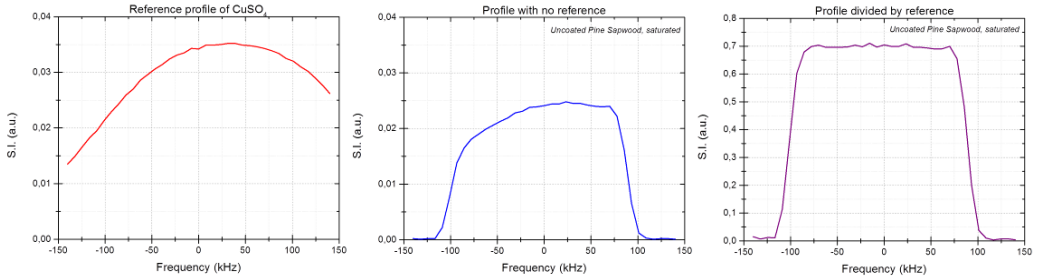

Figure 3-11: A visualization of the reference, the uncorrected profile and the corrected profile.

4 Optimization of the sample holder

This chapter presents the results of the measurements done with several setups. The setup is meant to compare coatings on wood. As what is expected, moisture transport through a coating on wood is much slower than transport without a coating. For examining the coatings for comparison, only moisture transport through the top of the sample must take place. To ensure that that is what is happening in the setup, two variables are considered. First, the influence of the sample holder is investigated and secondly the influence of covering the sides of the sample is researched.

4.1 Situation sketch of the sample holder

In Figure 4-1 (a), an illustration of the sample holder is shown. It is a hollow cylinder, with an inner diameter of approximately 19.95 mm and it has an inner height of 20 mm. The sample holders are made of impermeable Teflon. When the samples are saturated for drying measurements, the sample is swollen, as described in paragraph 2.4. For fitting these samples in the somewhat smaller sample holders, the holders are placed in an oven of approximately 105°C for circa 15 minutes. The sample holder will get a little bit more resilient so the sample can be pushed in more easily.

The sample can be coated, for the illustration this looks like darker wood. On the sides it is not coated, so this is lighter. Furthermore, on the top via the tube, dry air is blown in. It has an air flow of 3 liters per minute and it has an intended relative humidity of 0%, while it is actually ± 5%. On the top there are also small holes, so that the air can escape, with perhaps a higher humidity. Figure 4-1 (b) shows the air flow inside the sample holder.

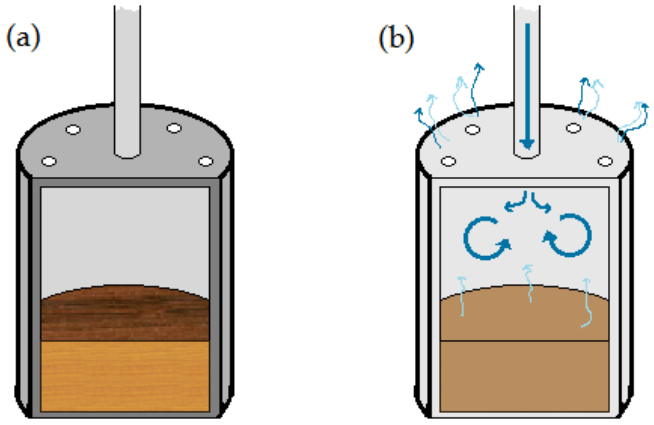

Figure 4-1: (a) an illustration of the sample holder, with a (coated) wood sample. (b) Shows the air flow inside the sample holder.

In Figure 4-2 is a more schematic representation shown of the different sample holders. (1) has a totally flat inside, (2) has a little inset at the height of the sample and (3) is the same sample holder as (2), only the sample has taped sides. The difference between (1) and (2) is discussed in section 4.2, in section 4.3 is the comparison between (2) and (3) made.

In Figure 4-3 is a schematic representation shown of the sample holders with the possible air flows. However, the drawn air flows from the samples are potential flows. With red and green is showed what is desired and what is not, if the air flow is there at all.

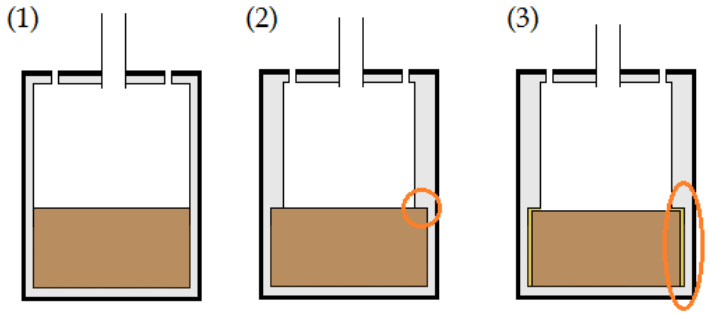

Figure 4-2: Schematic representation of the sample holders. (1) is completely flat on the inside, (2) has a little inset just above the sample and (3) is the same sample holder as b, only the sample is taped at the sides.

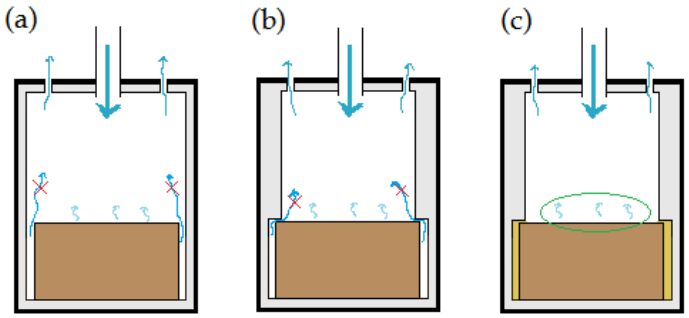

Figure 4-3: Schematic representation of the air flows in the sample holders. The shown air flows are potential air flows and with red and green is indicated what is desired and what is not.

4.2 Comparison of two kinds of sample holders

Measurements with sample holders (1) and (2), from Figure 4-2, are performed. With the flat sample holder (1), measurements are performed on Pine Sapwood with all the three coatings as described in paragraph 2.4. The inner diameter of the flat sample holder is d_{flat} = 19,95 mm. The total inner height is h_{flat} = 20 mm.

With the sample holder with an inset (2), measurements are done on Pine Sapwood with a solvent borne alkyd coating and a waterborne acrylic coating. The inner diameter of the bottommost part of the sample holder with an inset is also $d_{inset,bottom}$ = 19,95 mm, while the upper part has a diameter of $d_{inset,upper}$ = 18,95 mm. The height of both the parts is h_{bottom} = h_{upper} =10 mm.

For comparison, the measurements with both sample holders on the pine sapwood with a SB Alkyd coating and a WB Acrylic coating are used. In Figure 4-4 the profiles of the measurements are depicted. In figure 4-4 (a), the drying profile of the SB Alkyd coated pine in the flat sample holder is shown, in (b) the WB Acrylic coated pine.

Figure 4-4 (c) and (d) are the measurements with the sample holder with an inset and are respectively the SB Alkyd coated sample and the WB Acrylic coating.

These moisture content profiles are calculated with formula (1.20), from the signal intensity. The correction for the moisture contents below the FSP of 30%, as explained in the section of the calibration, is not done in these graphs. The difference between the M.C. and M.C.(NMR) is just a factor of 1.065 and is negligible here, because it won't change the time scale of the measurements. The influence of the decreasing bound water is really small in these measurements.

When looking by eye at the profiles and the time scales, a conclusion can already be drawn. The samples in the flat sample holder are dry in approximately 250 to 300 hours, while the samples in the other sample holder have lost only half of their moisture content in circa 550 hours. To substantiate this observation, the area under the MC profiles is plotted against the drying time in figure 4-4 (e) and (f). In Table 4-1 estimations of the drying times are given. For the second sample holder, a very rough linear extrapolation is used.

Table 4-1: Estimation of the drying times of Pine Sapwood with different coatings in two different sample holders.

Coating	Flat sample holder	Sample holder with inset
SB Alkyd	279 h ≈ 12 days	1050 h ≈ 33 days
WB Acrylic	299 h ≈ 13 days	1250 h ≈ 40 days

To give an idea about the actual duration of the drying, it is good to look at the measurements of van Meel [1]. He measured several types of wood, both with and without a coating. The uncoated woods took about 1 week for drying, while the coated woods dried in approximately one month. Comparing the values found in the measurements to the ones that van Meel found, it is easy to conclude that the flat sample holder is not sufficient for measuring the influence of coatings on the drying process. It seems as if the sample in the flat sample holder behaves like it is not coated. This could be explained by the shrinkage of the sample when it dries. The sides of the sample are not covered anymore and water will diffuse through the open sides. This also confirms the situation as outlined in Figure 4-3(a). The sample holder with an inset appears to provide the required situation as described in the introduction of this chapter.

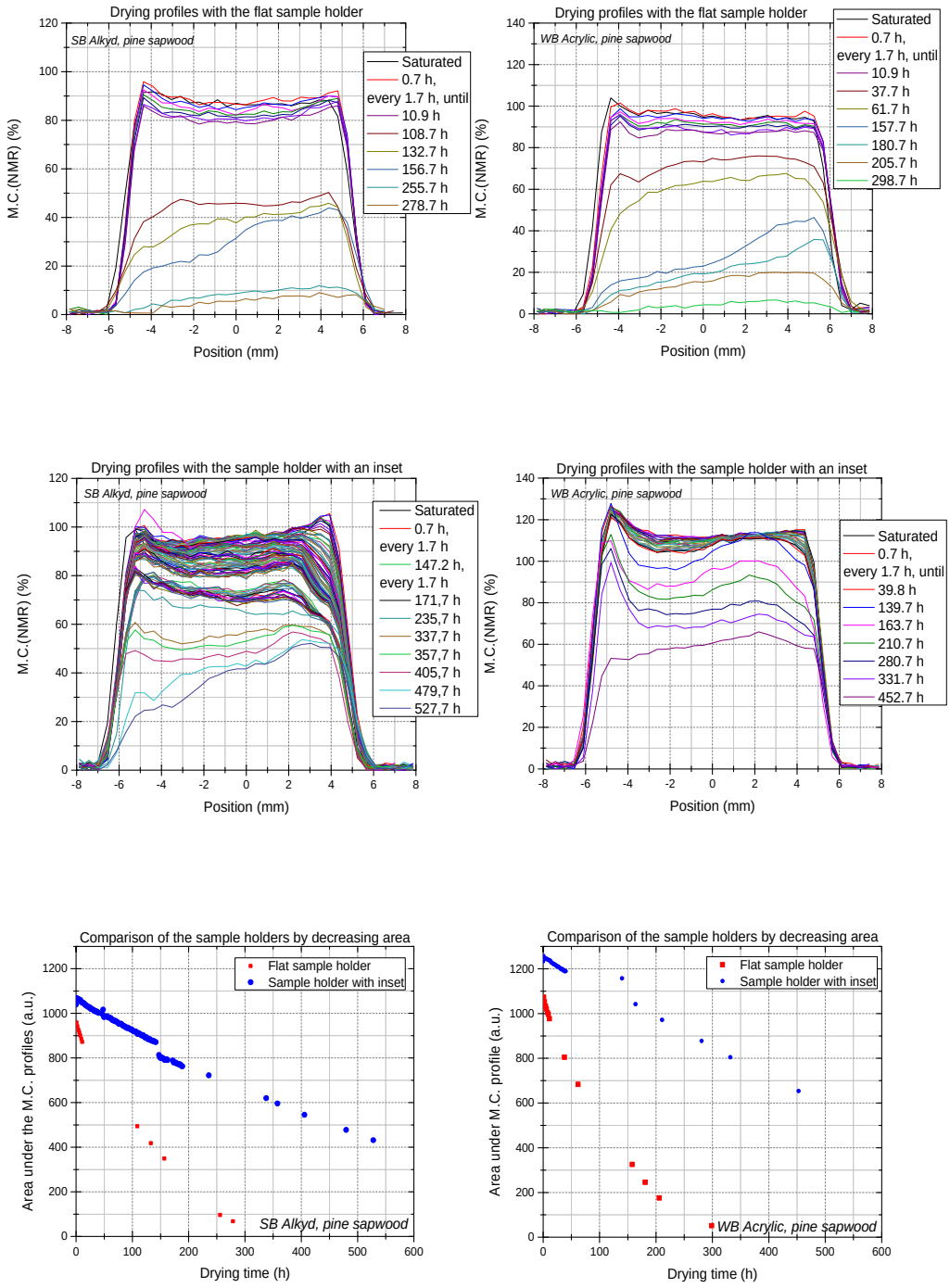

Figure 4-4: From left to right, from top to bottom (a) to (f). (a) Drying profiles with flat sample holder with SB Alkyd. (b) Flat sample holder, WB Acrylic, (c) sample holder with inset, SB Alkyd, (d) sample holder with inset, WB Acrylic, (e) comparison of the sample holders by integrating the profiles of SB Alkyd and WB Acrylic (f)

4.3 Comparison of a normal sample and an enclosed sample

The new question that comes up after the previous paragraph is whether the sample holder with inset is sufficient enough. Known is that when a new dry sample is saturated, it will swell with a maximum of 5% in the radial direction, as described in paragraph 2.4. For an oven dried Pine Sapwood sample, the sample has decreased in diameter to ± 19.55 mm. The upper inner diameter of the sample holder is 18.95 mm, so this should still prevent drying from the sides. However, the sample will also shrink in height, $h_{ovendried}$ = ± 9.84 mm. This means that when the sample dries, it will not stay against the inset and a small space will be created on top of the sample as sketched in Figure 4-3. The third situation will now be compared with the second. In figure 4-2 (3) is a schematic representation of the covered sample: the sides of the sample and a little bit of the top are covered with almost impermeable Teflon tape. A photograph from the situation can be seen in Figure 4-6.

The measurements are done with the same sample holder, the sample holder with the inset. The measurements are performed on two uncoated Pine Sapwood samples. One of them is not covered and has 'free sides', while the other one has tape around it and has 'taped sides'. The drying profiles of both these measurements are shown in Figure 4-5.

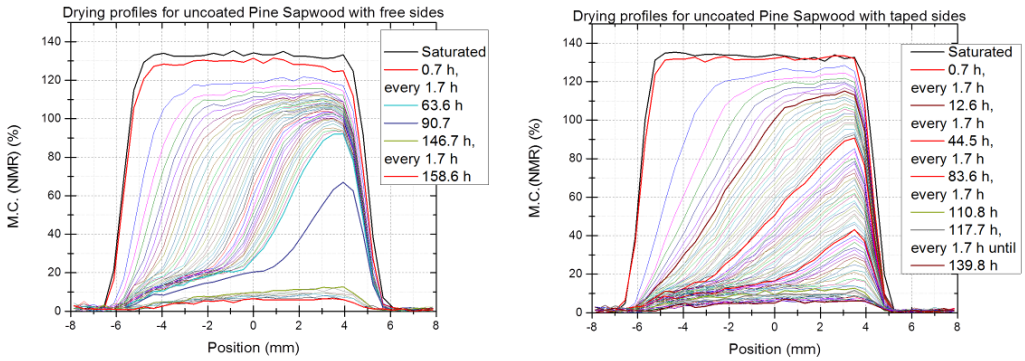

Figure 4-5: The drying profiles of uncoated pine sapwood. At the left is the sample with the free sides, on the right the sample with the taped sides.

What can be observed from Figure 4-6, is that the sample with the free sides has a sharper drying front than the sample that has taped sides. This may already indicate that the sample is sealed well enough without tape. An illustration of this argument is shown in Figure 4-6.

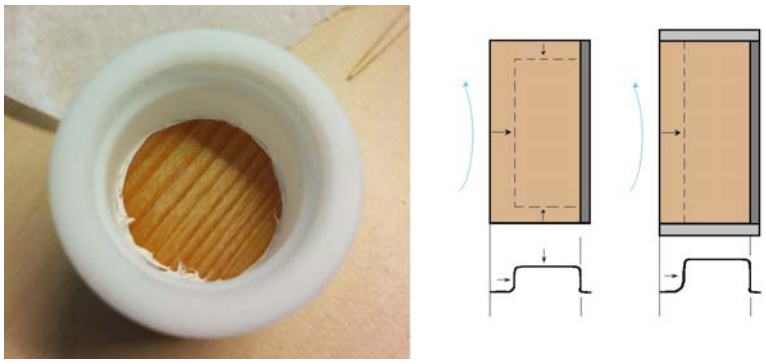

Figure 4-6: At the left a photograph of the sample covered in Teflon tape. On the top, the tape is pushed to the sides. At the right a schematic representation is shown with two situations. When the sample is sealed poorly, it will dry from all sides, except for the bottom. This will cause the drying front to be less sharp. When the sample is sealed good, it will only dry from the top and the drying front will be well defined.

In the right part of figure 4-6 two situations are drawn. When the sample is sealed poorly at the sides, the sample will dry from all the sides except for the bottom. This will cause the drying front to be poorly defined and less steep. However, when the sides are sealed good enough, the sample will only dry from the top and the drying front will therefore be well determined. Comparing these sketched situations to the measured profiles, this is indeed a hint that the sample with no tape is already covered correctly for obtaining information about the drying process and eventually about the coatings.

However, more proof must be provided. When comparing the area under the moisture content profiles through time, as is done with the coated sample in the previous comparison, the same behavior for both situations is observed. This can be found in Figure 4-7.

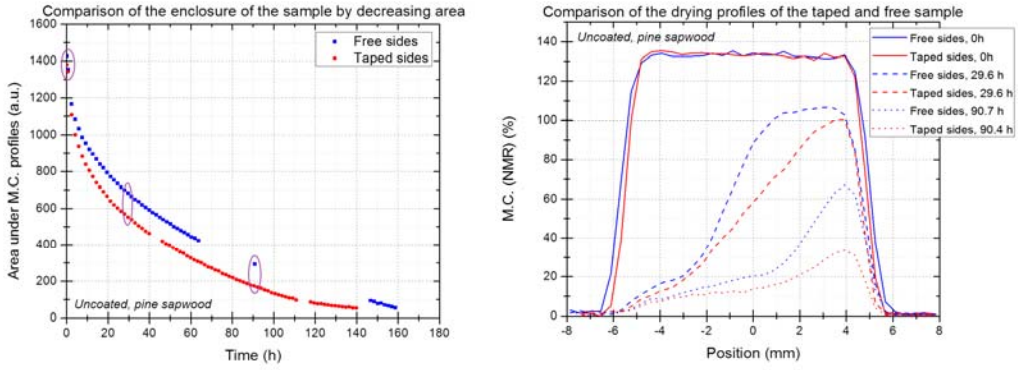

Figure 4-7: At the left the area under the moisture content profiles against time. Both the drying processes have the same shape, although the taped sample seems to have dried faster. At the right there are profiles at 3 steps in time, circled in purple on the left. That the shape of the drying front is different is clear.

What can be deduced from the figure that the area under the profiles decreases in a same way, only the taped sample was somewhat faster. At the purple circles, the profiles are drawn in the right part of figure 4-7. The first observation about the drying front is confirmed. Looking for example at the drying profiles after 29.6 hours of drying, the maximum moisture content is approximately the same, but the shape of the drying front is different.

Looking more accurately to the drying front is interesting at this point. The rate of the drying front, how fast it moves through the sample, can be compared. The time t=0 is the time when the saturated sample is measured, before the dry air is blown in. In these measurements, the drying front will occur after approximately 11 hours. A graph of this is showed in figure 4-8.

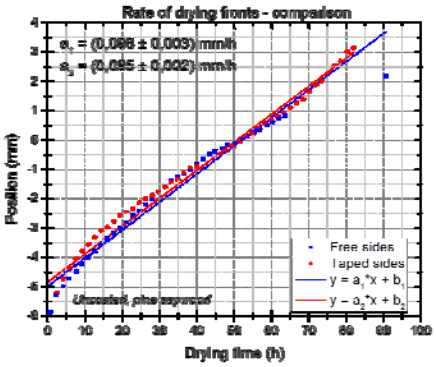

Figure 4-8: Comparison of the rate of the drying profiles. A rough linear approximation is made and both rates appear to be the same.

What can be seen in figure 4-8 is that the drying fronts behave the same in a linear approximation because the slopes coincide. However, it must be noted that after circa 70 hours of drying, the data points deviate. This is explicable: how drier a sample is, the more the internal structure per sample plays a role in the drying process Pictures of the structure on the outsides of the samples are taken and shown in Figure 4-9.

Figure 4-9: Pictures of the uncoated pine sapwood samples. U is the sample that was taped, K is the sample that had the free sides. Left: transverse section, right: tangential section.

What can be seen in the picture at the right is that the taped sample is not made with a clear radial cut but skew in comparison with free sample. This explains the difference in the drying front: for the free sample, the drying front passes all the longitudinal cells through pits. For the taped sample however, the drying front will move different at the left side of the sample in comparison with the right side of the sample because of the skew cut. The alignment of the cell walls and the pores is tilted relatively to the top of the sample. The type of moisture transport is now determined by a combination of transverse transport and radial transport, while the free sample only has transport in the radial direction. This was already explained in section 2.4. Because this deviation in structure, the assumption is that the drying front in both samples approximately behaves the same. For strengthening the argument that taping the sides is therefore not needed, more measurements should be performed on samples to compare the drying profiles and the influence of internal structure further.

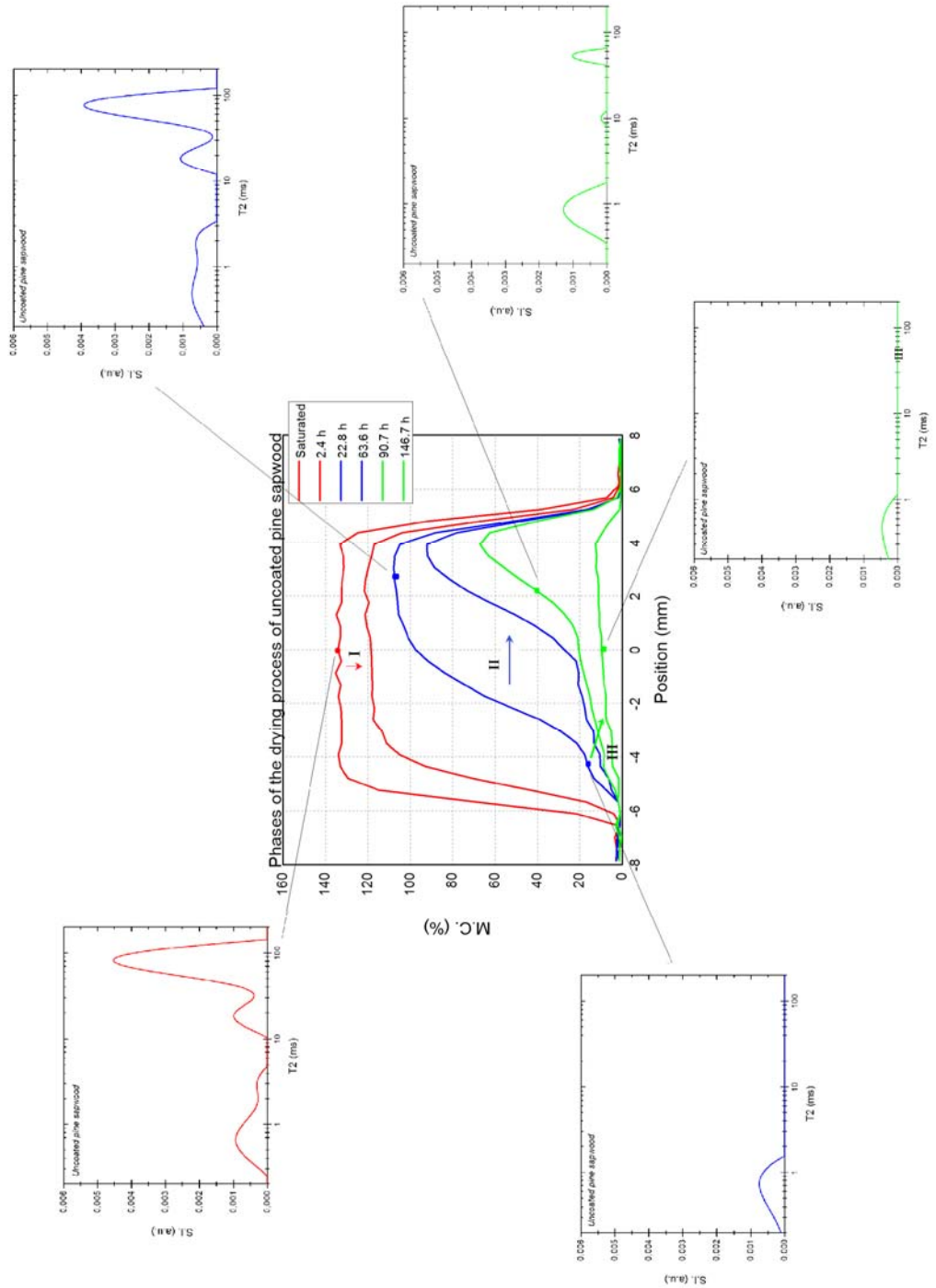

Figure 5: In the center, the phases of drying of pine sapwood are shown. On the sides, the associated T_2 – profiles are shown.

5 Raw model for the drying process of uncoated Pine Sapwood

For understanding the drying process of wood, in this case uncoated pine sapwood, it is useful to differentiate between the different phases that occur during the drying process. This differentiation with a physical explanation per phase is provided as a conceptual model in the first paragraph. In the second paragraph, a mathematical approach is taken towards the second phase of the drying process. The mathematical model will be compared with the measurements and all the similarities and deviations will be discussed.

Eventually, such a model can be applied to perhaps coated pine sapwood, or on other types of wood. This will provide another method of comparing measurements on wood and coatings, or it can clarify differences in structure of several types of wood.

5.1 Conceptual model

Phase I: The first stage is the homogeneous drying of the sapwood. This is probably due to the fact that the cells and pores are connected and aligned when saturated. Therefore, the drying process is not limited by the wood but by the external environmental conditions. A schematic representation is shown in Figure 5-1.

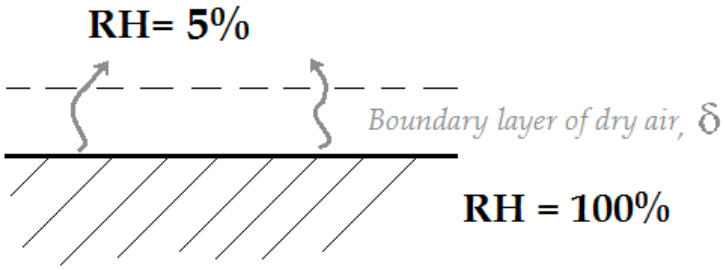

Figure 5-1: Schematic representation of the top of the sample with environmental conditions.

The sample has a relative humidity of 100% and the dry air blown in will create a boundary layer with thickness δ with a RH of approximately 5%. This gradient in vapor density will cause diffusion D of the water. So the evaporation rate E is limited by these conditions, together with the area A. This can all be caught in one formula,

$$E \approx A \cdot D_{water,air} \cdot \frac{\Delta \rho_{w,vapor}}{\delta} \tag{1.23}$$

For other wood types, for example teak, this phase doesn't exist. For pine sapwood, almost all pores are connected and filled with water. During the first parts of drying, the pores will be disconnected because some of them will become empty, which will start the drying front of phase II. For teak, the pores were never aligned, so a drying front will form immediately. So this phase depends highly on the porosity and the geometry of the wood sample. A comparison of these internal structures can be seen in Figure 5-2.

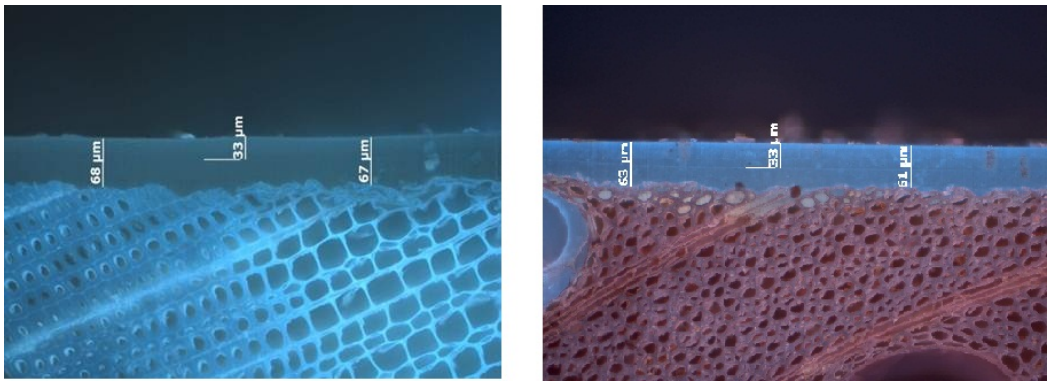

Figure 5-2: Optical microscope pictures of; Left: pine sapwood (with a SB Alkyd coating). Right: Teak (with a WB Alkyd coating).

From these optical microscope pictures the internal structure can be compared for the teak and pine. For the pine sapwood, the cells are all aligned and the cell walls are all aligned. For teak, the structure is not only denser, but there is no order in the structure of the cell walls. This explains why this homogeneous phase occurs at pine sapwood and not with teak.

As can be seen on the sides of Figure 5, the T_2-profiles of the homogeneous drying profiles include the free water. Free water has a long relaxation time due to the difference in spin-spin interaction compared to the bound water. In the red T_2 profile, at higher T_2 (above 10 ms), large peaks appear. During the homogeneous drying, these peaks will decrease first; in the red T_2-profile the maximum S.I. is 0.0045, in the blue one with free water it is 0.0039 and for the green one halfway the drying front, the free water has a S.I. of 0.001.

Phase II: The second phase of the drying process is the movement of the formed drying front. In paragraph 4.3, these drying fronts are already discussed. The shape and speed of the drying front were already considered. In the next paragraph, the mathematical model will go deeper into this.

It is however interesting to look at the T_2 profiles. On the wet part of the front, free water is still present at the higher relaxation times. Though halfway of the front, it is clear that a decrease in the free water is observed. The green profile on the right in Figure 5 shows this. The driest part of a profile with a front only includes the bound water, shown in a green profile on the left. The dry part of the drying front will have approximately the same amount of bound water, while the free water in the wet side decreases first. After all the free water has disappeared, the bound water will decrease, which is phase III.

Phase III: The third and last phase of the process is the decrease of bound water in the sample. It will start to decrease when the free water has already left. The fiber saturation point FSP must be taken into account. From that point, when bound water will disappear, the sample will also shrink because the individual cells will shrink when they lose bound water. This shrinking is described in paragraph 2.2 and shown in Figure 2-4, the sorption isotherm. The FSP for pine sapwood is around 30% of moisture content. When looking at the dry part of phase II, this already is a little bit under the FSP.

The relaxation times for the bound water are very low, they are smaller than 10 ms. When comparing the maximum T_2-value of the bound water of the green T_2-profiles and the dry part of the blue profile in Figure 5, it can be observed that the relaxation time shifts to the left during drying. For the green profile with some free water, $T_{2,max}$ = 0,88 ms, for the blue profile it is $T_{2,max}$ = 0,73 ms and for the green profile with only bound water: $T_{2,max}$ = 0,47 ms. These values make clear that the less moisture is present, the lower is the T_2-value. This can be explained with the fact that clusters of bound water will disappear and more tight bound water will stay longer, as stated and shown in paragraph 3.2.2.

What also can be observed in these profiles is that some signal is lost due to the low T_2 –times. The used setup can't have a shorter echo time, so not all the signal can be measured. The repetition time could however be decreased for the measurements of this phase. By this, the averaging can be higher and the signal to noise ratio will be better, which really affects these profiles because of their low signal intensity.

5.2 Raw mathematical model

For the mathematical model, a physical approach has been taken. For the explanation, a schematic representation is shown in Figure 5-3.

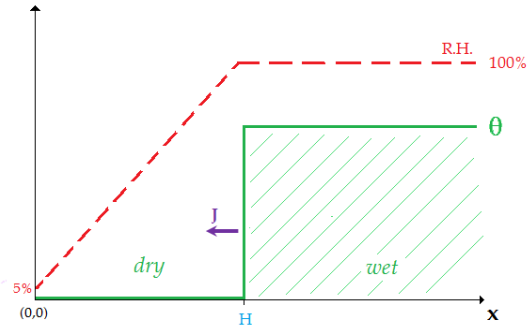

Figure 5-3: A schematic representation of the model.

As can be seen in the representation, the approximation is that the drying front has a completely dry part and a completely wet part. The position of the drying front is denoted as H. H_0 is defined as the top of the sample and is set to zero in respect to H. What physically happens is that a volume of water is disappearing in the wood, which is equal to the flux of the diffusion over the area. The flux of the diffusion is denoted as J and can be described by Fick's law. This approach eventually leads to the next differential equation:

$$\theta \cdot \frac{dH}{dt} = D \cdot v \frac{\Delta\rho}{H} \qquad (1.24).$$

In this formula is θ the amount of moisture per volume and dH/dt describes the movement of the drying front. This change of volume of water is equal to the diffusion of the water due to the difference in vapor pressure divided by the position $\Delta\rho/H$. One of the assumptions in this model is that $\Delta\rho/H$ is constant, what can be seen in the figure of the model as the linear decrease of the relative humidity.

Assumed is also that the diffusion coefficient D is constant during the drying process and that the R.H. inside the sample in the wet part of the drying front is always 100%. The complete derivation of the equation above is described in Appendix A.

The found differential equation can be easily solved. Equation (1.25) is for checking if the rate of the drying fronts can be described with this formula, therefore (1.24) is rewritten:

$$H^2 = \frac{2Dv \cdot \Delta\rho}{\theta} t + \left[H_0^2 - \frac{2Dv \cdot \Delta\rho}{\theta} t_0 \right] = a_{slope} \cdot t + b \tag{1.25}$$

As already mentioned above is H_0 = 0, the top of the sample. H will therefore be between 0 and 10 mm. t_0 is also taken as 0, which is the time at which the saturated profile is measured. It is clear from this equation that the square of the position of the drying front is linear to the time.

The diffusion coefficient can now easily be determined with the slope of the previous linear approximation, by just rewriting:

$$D = \frac{a_{slope} \cdot \theta}{2v\Delta\rho} \tag{1.26}$$

This mathematical model is now applied to the previous measurements of the uncoated pine sapwood. First, the model is applied to the behavior of the drying front to calculate the diffusion coefficient D. Secondly, the model is compared with individual profiles.

5.2.1 Applying the model to the behavior of the drying front

In this section, the model is compared with the rate of the drying fronts, already seen in section 4.3. The free parameters in the model for this comparison are the position H, and the time t, at a constant amount of water θ. The model is applied to the data of figure 4-8 and this data is converted to H^2 against the time t, with the H_0 and t_0 as described above. These figures are shown in Figure 5-4.

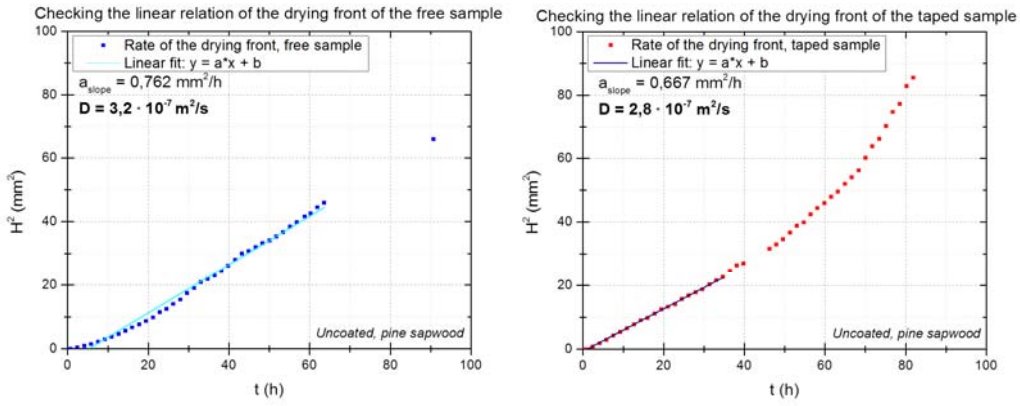

Figure 5-4: The drying fronts of the free (left) and taped (right) sample, in H^2 against t. The slope gives information about the diffusion coefficient D.

The fronts in the figure are linearly fitted as stated in equation (1.25). However, not the complete range of data points is fitted. The reason for that is that the drying front will reach the bottom of the sample at a certain point and the model cannot be applied anymore: the assumption that there is a completely dry and wet part doesn't hold, because when the drying front has reached the bottom, the completely wet part will dry as well. For the free sample is the last profile that didn't reach the bottom is the one after 63.6 hours of drying. For the taped sample this is a lot quicker, it is after 34.7 hours of drying.

However, if the linear fit is compared with the data, there are still some deviations. For the free sample for example, the first 5 to 10 points are also not really in the linear regime. But that makes sense when the definition of t_0 is taken into account: it is the time when the saturated sample is measured. Due to the first phase of homogeneous drying, it takes some time before the drying front comes in. So the first few points don't belong to the drying front. For the taped sample, the points after the 34.7 hours of drying deviate a lot from the linear fit. This is probably due to the structure of the sample as already explained in section 4.3.

The linear approximation of the model is however similar to the data points. The question is now if the linear fit returns a realistic diffusion coefficient. These are respectively Dfree = $3{,}2*10^{-7}$ m²/s and D_{taped} = $2{,}8*10^{-7}$ m²/s. The diffusion coefficient of free water in air is $D_{w,air} = 2.4 * 10^{-5}$ m²/s, [13]. The self –diffusion of water is $D_{w,water}$ = $2{,}3 * 10^{-9}$ m²/s, [14]. It is clear that the diffusion that takes place is vapor diffusion. It is however, two powers of ten slower than that for water in air. This is understandable if the schematic representation of a cell with water is considered, as in figure 5-5.

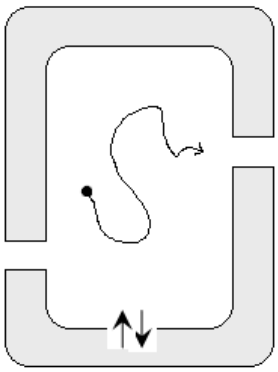

Figure 5-5: A schematic representation of a cell and the interaction of water.

From the figure can be deduced that the evaporation is slowed down because of the smaller exits in the cell wall; for a lot of cells together, this will lower the diffusion coefficient with respect to pure vapor diffusion. Water molecules also will absorb and desorb from cell walls, during the process of drying, and this will also cause delay in the vapor diffusion process.

The found diffusion coefficients in the measurements after applying the model are realistic and credible values if the interaction of water with wood is taken into account.

5.2.2 Comparing the model to individual profiles

In this comparison, the free parameters are θ and *H*, while the time t is a constant now. This just provides another approach for comparing the model with the measurements and check for similarities and deviations.

The individual profiles that are compared are a saturated profile of the free sample and the drying profiles after 29.6 hours of drying for both the free and taped sample. In Figure 5-6(left), the three profiles are shown. The saturated profile is just to show the assumption that the R.H. is 100% inside the wet part of the sample. The profiles after 29.6 hours are chosen because the drying front is approximately halfway and has not reached the bottom of the sample yet. The moisture content profiles are first corrected below the FSP, as explained in the calibration in section 3.2.3. After this correction, they are converted to relative humidity profiles with the sorption isotherm. These R.H. profiles are shown in Figure 5-6 (right)

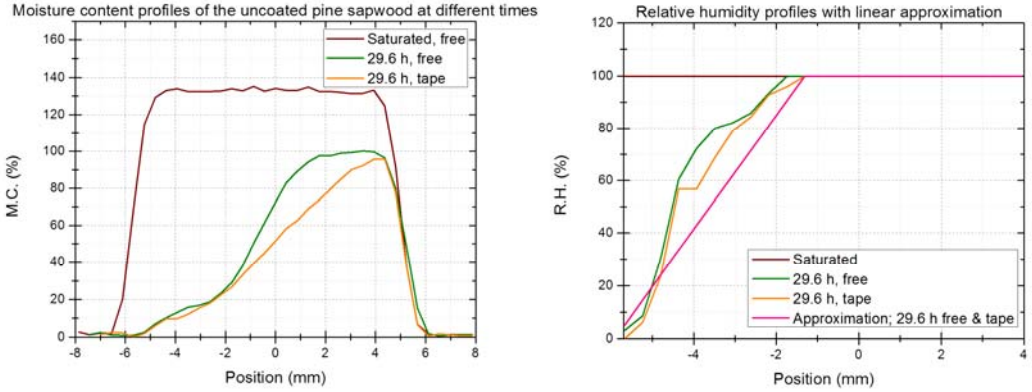

Figure 5-6: Left: Corrected M.C. profiles for M.C. below FSP. Right: R.H. profiles with the linear approximation in pink.

The assumption of the model is that $\Delta\rho/H$ is constant, which means that ρ_{wet}-ρ_{dry}/H is constant. However, this is just a first order approximation. So the relative humidity will increase linearly until it reached the drying front. It is remarkable that both the free and taped sample show the same curved behavior, though the model is linear.

However, the diffusion seems slower near the drying front and faster near the dry top of the sample. So the overall behavior can be seen as linear. The deviation could nevertheless be due to the assumption that the diffusion coefficient is constant during the process. But if the drying front is more at the top of the sample, the water diffuses to a small volume of wood. But when the drying front has almost reached the bottom, the water vapor must travel al long way to the top of the sample and the interaction with the wood is much more intensive. This would explain the quicker diffusion at the top and the slower diffusion at the bottom.

The comparisons made in this chapter can be summarized in a schematic representation, as shown in Figure 5-7.

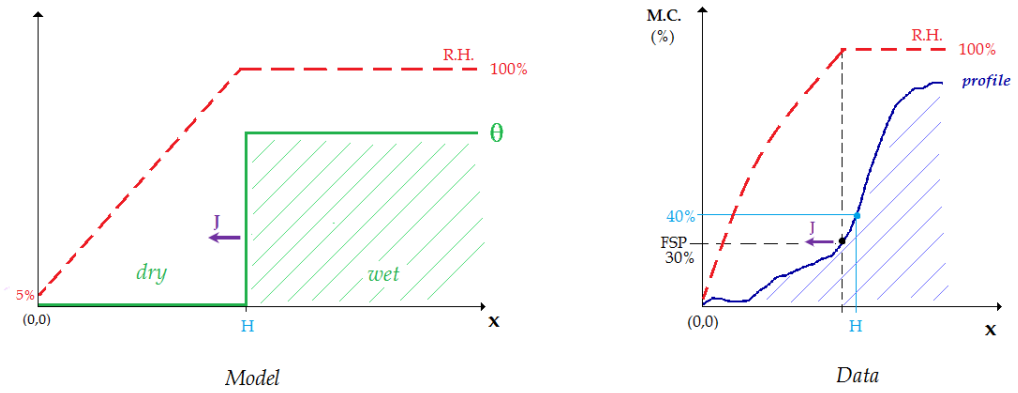

Figure 5-7: Left: The model with the assumptions, Right: Data.

Where the assumption is that the R.H. increases linearly, it actually shows a curved behavior as discussed above. Also, the position of the drying front is hard to define because the drying front isn't that steep. For the comparison, the position is taken at 40% M.C., but the really dry part in the model is actually the bound water in the real data. When the comparison is done at the FSP and the signal is corrected for the bound water, the model should be more similar to the data. What then must be kept in mind is that the sorption isotherm can't be used after the correction.

For the really simple mathematical model, it gives acceptable results when comparing them to the data. The deviations however, are due to the assumptions.

6 Conclusions and recommendations

6.1 Conclusions

First, there can be concluded that NMR techniques are excellent for measuring drying processes of wood in a non-destructive way. Various profiles have been made and the used sequences provide enough information about the T_2 relaxation times.

As can be concluded for optimization of the sample holder, is that the right kind of sample holder is found. The sample holder needs to have a narrower upper part of 18.95 mm for a good enclosure of the sample. When a flat holder is used, the sample will dry too quickly because the sides are not covered after a little shrinkage of the sample. This way, the influence of coatings on the drying process can never be compared.

Secondly, when the right sample holder is used, the sample is probably correctly enclosed. This conclusion can be drawn from the comparison of two uncoated pine sapwood samples of which one is taped on the sides with Teflon and the other is not. The difference in the drying profiles and the small difference in the rate of the drying front are due to the internal structure of the wood: the taped sample was cut skew relatively to the radial direction.

For the modelling part there can be concluded that the conceptual model of the drying process consists of three phases: first the homogeneous drying, which doesn't occur for teak. The evaporation in this phase is limited by the boundary layer of dry air on top of the sample. The second phase is the phase which describes the shape and movement of the drying front. The third and last phase is the phase of the decrease of the bound water and therefore the shrinkage of the sample. In this phase, T_2-analysis shows the shift of the relaxation time due to loss of clusters of bound water while tight bound water will be bound longer.

When the mathematical model is applied to the behavior of the drying front, a linear fit can be made from H^2 against t. However, this can only be done when the drying front hasn't reached the back of the sample yet. This fitting yielded diffusion coefficients of D_{free} = 3,2*10^{-7} m^2/s and D_{taped} = 2,8*10^{-7} m^2/s. This is slower than just vapor diffusion of air, but that can be explained by the interaction of water in wood.

When the model is compared to individual profiles, the data deviates a little from the model. The model shows a linear behavior, while the data shows a more curved behavior. This is probably due to the fact that the diffusion coefficient is not constant while the drying front is passing, because of the interaction of water with wood. However, when averaging the curved behavior, the linear approximation seems to fit.

6.2 Recommendations

A correct setup is now available, but the measurements can be improved. For measuring drier samples, the same parameters are used as for really wet samples, which lead to inaccurate data. It is inaccurate because the signal intensity is then in the same region as the noise. For a better description of the third phase of drying, the parameters should be optimized. The repetition time can be shortened and the averaging can therefore be larger: the SNR can be improved.

Furthermore, a good insight on the internal structure of wood may provide information about deviations in drying processes. The difference in the front of the uncoated samples for example, is a result of difference in geometry. CT-scans of the samples will provide information about the geometry and porosity, which helps interpreting results.

For improving the model, a lot of work can be done. Looking at structure of wood and the interaction of water with wood will give a better insight in the drying process. This interaction could give hints for a changing diffusion coefficient during the drying process.

Acknowledgements

Without support from many people, I wouldn't have managed to finish the project. Therefore, I'd like to thank the ones who were there for me.

First, I'd like to thank Özlem. You're a wonderful supervisor. Although you were abroad during the beginning of my project, you still managed to supervise me through email. This was also good for me, I've learned how to do research on my own. When you were back, you were always there for me. If I had questions, you always took the time to explain things to me. You work well structured and I can still learn from that. I liked working together with a chemist, because at some points you had a complete other thinking pattern than me. I find that very inspiring. Nevertheless, I also enjoyed the chats about things that had really nothing to do with the project.

Secondly, I'd like to thank Henk, also my supervisor. I loved the meetings we had once a two weeks. You are a really good teacher and I enjoyed gaining knowledge about physics from you. The discussions about my work were good and I could really do something with the feedback. Thanks a lot!

Additionally, I'd like to thank the people in the TPM group. Pim, Karel and Kees always answered my small questions and were always willing to help me. Okan, thank you for the deal we made about the window and the door. For the rest of the group; I enjoyed spending my time here in 2,5 months. Bedankt voor de gezelligheid!

References

[1] P.A. van Meel, *Moisture transport in coated wood*. TNO-report, October 2009

[2] P.A.J. Donkers, *the effect of coatings on the moisture uptake of wood: an NMR study*, *TU/Eindhoven*, October 2010

[3] R.S. Menon *et al.*, A*n NMR Determination of the Physiological Water Distribution in Wood during Drying*, 1987

[4] P. Wiberg *et al.*, *Heat and mass transfer during sapwood drying above the fiber saturation point,* 2000

[5] S.J. Hill *et al.*, *Effect of drying and rewetting of wood on cellulose molecular packing*, 2010

[6] M.A. Stanish *et al., A mathematical model of drying for hygroscopic porous media,* 1986

[7] University of Cambridge, *Dissemination of IT for the Promotion of Materials Science*, June 14 2014,

http://www.doitpoms.ac.uk/tlplib/wood/printall.php

[8] Arno, J., *Encyclopedia of Wood. Time-Life Books*, 1993

[9] F. Bulian & J.A. Graystone, *Wood Coatings, theory and practice*, Elsevier, 2009, Chapters 6 & 10

[10] Dr. J.P Hornak, *The Basics of MRI*, 1996 – 2014, Chapters 3, 4, 6, 8 & 12

http://www.cis.rit.edu/htbooks/mri/inside.htm

[11] C.D. Arauju *et al.*, *Proton magnetic resonance techniques for characterization of water in wood: application to white spruce*, 1992

[12] R.S. Menon *et al.*, *Quantative Separation of NMR Images of Water in Wood on the basis of* T_2, 1989

[13] Isodoro Martínez, *Mass Diffusivity Data*, 1995-2014,

http://webserver.dmt.upm.es/~isidoro/dat1/Mass%20diffusivity%20data.pdf

[14] M. Holz, S.R. Heil, A. Sacco: *Temperature-dependent self-diffusion coefficients of water and six selected molecular liquids for calibration in accurate 1H NMR PFG Measurements*. In: *Phys. Chem. Chem. Phys.* 2, 2000, S. 4740–4742.

Appendix A – Derivation of Fick's model

For describing moisture transport in porous material, the following equation is essential:

$$\theta \cdot A \cdot \frac{dH}{dt} = -A \cdot v \cdot J \tag{1.27}$$

Θ is the amount of water per volume, *A* is the surface area and together with dH/dt it gives the change of the volume. The whole left side is the volume of water that is evaporating. At the right side *v* is the volume of water per mol and *J* is the flux of the diffusion. The next needed formula is Fick's law:

$$J = -D\frac{d\rho}{dH} \tag{1.28}$$

Where *D* is the diffusion coefficient and dρ/dx is the gradient in the vapor density which causes the diffusion. Combining the two equations give a differential equation:

$$\theta \cdot \frac{dH}{dt} = D \cdot v\frac{d\rho}{dH} = D \cdot v\frac{\Delta\rho}{H} \tag{1.29}$$

Applying the separation of variables technique gives

$$\int HdH = \int vD\frac{\Delta\rho}{\theta}dt \tag{1.30}$$

Which leads to an equation for the diffusion coefficient:

$$D = \frac{H^2\theta}{2v\Delta\rho t} \tag{1.31}$$

Δρ can be determined because the relative humidity is known, as is the saturation vapor density. The assumption is however, that the relative humidity is 100%. Θ is the moisture content divided by 100. That is the moisture content where the drying front is considered. Both *H* and *t* are variables measured by the data. Another assumption that is made is that the entire signal is received. No extrapolation is used in the drier profiles.

Checking if the raw model fits the data, the derivation is a little bit different. Assume

$$\frac{dH}{dt} = \frac{C}{H} \tag{1.32},$$

Where C is a constant, existing of the other parameters and especially *D* can be deduced from *C*.

$$\begin{aligned} dH^2 &= 2Cdt \\ H^2 - H_0^2 &= 2C(t - t_0) \\ H^2 &= 2Ct + \left[H_0^2 - 2Ct_0\right] \end{aligned} \tag{1.33}$$

The last formula is easy to check with the data, when H_0 and t_0 are chosen wisely.

Appendix B – Handmade scripts

For loading the collected data in Origin 9.0, two import scripts are written. One for converting the information to signal intensity, and the other to moisture content.

For S.I.:

```
del col(1);
wtranspose;
col(2)=col(1)/17,82;
del col(1);
wks.col1.type=4;
col(1)[L]$="Position";
col(1)[U]$="mm";
col(2)[L]$="S.I.";
col(2)[U]$="(a.u.)";

plotxy (1,2:end) plot:=200;
```

And for M.C.:

```
del col(1);
wtranspose;
col(2)=col(1)/17,82;
del col(1);
wks.col1.type=4;
col(1)[L]$="Position";
col(1)[U]$="mm";
col(2)[L]$="M.C.(NMR)";
col(2)[U]$="(%)";

for( int ii = 2 ; ii <= 100 ; ii+=1)
{
  wcol($(ii))=1000*(100*(wcol($(ii)))*10^-6*pi)/(1649.73*10^-6);
}
plotxy (1,2:end) plot:=200;
```